Lie Optimal Solutions of Heat Transfer in a Liquid Film over an Unsteady Stretching Surface with Viscous Dissipation and External Magnetic Field

Haris Ahmad

Reg No # 00000361708

Supervisor

Dr. Muhammad Safdar

Department of Mechanical Engineering

School of Mechanical and Manufacturing Engineering (SMME)

National University of Sciences and Technology (NUST)

Islamabad, Pakistan

April 2023

Lie Optimal Solutions of Heat Transfer in a Liquid Film over an Unsteady Stretching Surface with Viscous Dissipation and External Magnetic Field

Author

Haris Ahmad

Reg No # 00000361708

A thesis submitted in partial fulfillment of the requirements forthe degree of MS Mechanical Engineering

Thesis Supervisor:

Dr. Muhammad Safdar

Thesis Supervisor's Signature:_____

Department of Mechanical Engineering

School of Mechanical and Manufacturing Engineering (SMME)

National University of Sciences and Technology (NUST)

Islamabad, Pakistan

April 2023

FORM TH-4

MASTER THESIS WORK

We hereby recommend that the dissertation prepared under our supervision by:

Name: Haris Ahmad

Reg # 00000361708

Titled: "**Lie Optimal Solutions of Heat Transfer in a Liquid Film over an Unsteady Stretching Surface with Viscous Dissipation and External Magnetic Field"** be accepted in partial fulfillment of the requirements for the award of MS Mechanical degree.

Examination Committee Members

1. Name: Dr. Zeeshan Saeed Signature: _____

2. Name: Dr. Muhammad Umar Farooq Signature: _____

3. Name: Dr. Hina Munir Dutt Signature: _____

Supervisor's name: Dr. Muhammad Safdar Signature: _____

Date: _____

_____ _____

Head of Department Date

COUNTERSINGED

Date: _____ _____

Dean/Principal

THESIS ACCEPTANCE CERTIFICATE

Certified that final copy of MS/MPhil thesis written by **Haris Ahmad**, Registration number: **00000361708** of SMME has been vetted by undersigned, found complete in all aspects as per NUST Statutes/Regulations, is free of plagiarism, errors, and mistakes and is accepted as partial fulfillment for award of MS degree. It is further certified that necessary amendments as pointed out by GEC members of the scholar have also been incorporated in the said thesis.

Supervisor signature with stamp: _____

Supervisor Name: **Dr. Muhammad Safdar**

Date: _____

HOD signature with stamp: _____

Date: _____

Countersign by:

Dean/Principal signature: _____

Date: _____

Certificate for Plagiarism

It is certified that MS Thesis Titled "**Lie Optimal Solutions of Heat Transfer in a Liquid Film over an Unsteady Stretching Surface with Viscous Dissipation and External Magnetic Field**" by **Haris Ahmad, Reg # 00000361708** has been examined by me. We undertake the follows:

a. Thesis has significant new work/knowledge as compared already published or are under consideration to be published elsewhere. No sentence, equation, diagram, table, paragraph, or section has been copied verbatim from previous work unless it is placed under quotation marks and duly referenced.
b. The work presented is original and own work of the author (i.e., there is no plagiarism). No ideas, processes, results, or words of others have been presented as Author own work.
c. There is no fabrication of data or results which have been compiled/analyzed.
d. There is no falsification by manipulating research materials, equipment or processes, or changing or omitting data or results such that the research is not accurately represented in the research record.
e. The thesis has been checked using TURNITIN (copy of originality report attached) and found within limits as per HEC plagiarism Policy and instructions issued from time to time.

Name & Signature of Supervisor

Dr. Muhammad Safdar

Signature**:**_____

Declaration

I *Haris Ahmad* certify that this research work titled “Lie Optimal Solutions of Heat Transfer in a Liquid Film over an Unsteady Stretching Surface with Viscous Dissipation and External Magnetic Field” is my own work. The work has not been presented elsewhere for assessment. The material that has been used from other sources has been properly acknowledged/referred.

_____

Haris Ahmad,

Reg No #
00000361708

Date: _____

Copyright Notice

- *Copyright in text of this thesis rests with the student author. Copies (by any process) either in full, or of extracts, may be made only in accordance with instructions given by the author and lodged in the Library of SMME, NUST. Details may be obtained by the Librarian. This page must form part of any such copies made. Further copies (by any process) may not be made without the permission (in writing) of the author.*

- *The ownership of any intellectual property rights which may be described in this thesis is vested in SMME, NUST, subject to any prior agreement to the contrary, and may not be made available for use by third parties without the written permission of SMME, which will prescribe the terms and conditions of any such agreement.*

- *Further information on the conditions under which disclosures and exploitation may take place is available from the Library of SMME, NUST, Islamabad*

Acknowledgments

I am thankful to my Creator Allah Subhana-Watala to have guided me throughout this work at every step and for every new thought which You setup in my mind to improve it. Indeed I could have done nothing without Your priceless help and guidance. Whosoever helped me throughout the course of my thesis, whether my parents or any other individual was Your will, so indeed none be worthy of praise but You.

I would like to express my sincere gratitude to my supervisor Dr. Muhammad Safdar, who always made me feel excited about my work. The edification and brace that he gave me truly helps the progression and smoothness of my research work. Your insightful feedback pushed me to sharpen my thinking and brought my work to a higher level. Truly speaking, this thesis could not be possible without your guidance and teaching. Besides my advisor, I am also gratified to my Guidance and Examination Committee (GEC) members, Dr. Zeeshan Saeed, Dr. Muhammad Umar Farooq and Dr. Hina Munir Dutt, for their valuable instructions, helpful suggestions, and insightful comments.

I convey my deep heart rooted thanks to my parents, for their never-ending love, prayers, encouragement, and support and advise me to trust Allah and believe in hard work.

Haris Ahmad

Dedication

I want to dedicate my thesis to my beloved parents, my brother and my wife who have always been there for me throughout the degree.

Abstract

In this thesis, we explore the fluid flow and heat transfer in thin liquid films over an unsteady stretching surface with viscous dissipation under the influence of an external magnetic field. To investigate the behavior of this system, we use similarity transformations with the analytical and numerical solution techniques. Specifically, we derive the Lie point symmetries of the system of partial differential equations that describes the flow and heat transfer in a thin liquid layer. A 5-dimensional Lie point symmetry algebra is derived. We develop new similarity transformations for the given model using a pair of the admitted Lie point symmetry generators. Arbitrary coefficients are used in the Lie optimal system and these arbitrary coefficients may be employe to the control the flow and heat transfer.

By constructing the optimum system of Lie sub-algebras, related invariants, and similarity transformations, we reduce the number of independent variables in this flow model and convert the partial differential equations into ordinary differential equations for simplifying the solution procedure. This conversion requires double reduction, and the resulting transformations allow us to reduce the model to nonlinear ordinary differential equations.

To examine the proposed magnetohydrodynamic (MHD) flow and heat transfer, we build analytic solutions for the obtained system of ordinary differential equations using the Homotopy analysis approach. The results are presented in the form of tables and figures, which demonstrate how the magnetic parameter, Prandtl number, Eckert number, and unsteadiness parameter affect fluid velocity, film thickness, and heat transfer. We compare these changes in velocity and temperature profiles with those previously reported for flow and heat transfer inside a thin film under the influence of viscous dissipation and an external magnetic field.

Overall, our findings provide valuable insights into the behavior of fluid flow and heat transfer in thin films over unsteady stretching surfaces with viscous dissipation and external magnetic fields. These insights have important practical applications in fields such as chemical engineering, material sciences, and energy transfer.

Table of Contents

List of Figures

List of Tables

Chapter 1. Introduction

1.1 Background and Motivation

Heat transfer in a liquid film over an unsteady stretching surface is a complex and challenging problem with many practical applications in various industrial and biomedical fields. The understanding of heat transfer in such systems is crucial for the design and optimization of heat transfer systems. Viscous dissipation and an external magnetic field have been shown to have significant effects on heat transfer and fluid flow in a liquid film over an unsteady stretching surface. For instance, in a recent study [8], the influence of viscous dissipation and a magnetic field on heat transfer and fluid flow in a liquid film over an unsteady stretching surface is investigated. The study found that the presence of viscous dissipation and a magnetic field significantly impacted the heat transfer and fluid flow characteristics in the liquid film. Therefore, studying the effects of viscous dissipation and a magnetic field on heat transfer in thin liquid films over an unsteady stretching surface is an important area of research.

In recent years, Lie symmetry analysis has emerged as a powerful tool to study and analyze fluid flow and heat transfer in thin films over unsteady stretching surfaces. In this study, we derived the Lie point symmetries for a system of partial differential equations describing the flow and heat transfer in a thin liquid layer over an unsteady stretching surface with viscous dissipation in the presence of an external magnetic field. A 5-dimensional Lie point symmetry algebra is obtained, and we used linked invariants to develop new similarity transformations for the given model using a pair of the admitted Lie point symmetry generators. These transformations allowed us to reduce the number of independent variables of this flow model and convert the partial differential equations into ordinary differential equations, thus simplifying the solution procedure.

To examine the proposed MHD flow and heat transfer, we constructed analytical solutions for this system using the Homotopy analysis approach. The findings of this study are provided in the form of tables and figures, showing how the magnetic parameter, Prandtl number, Eckert number, and unsteadiness parameter affect fluid velocity, film thickness, and heat transfer. Our results indicate that the presence of an external magnetic field, along

with viscous dissipation, has a significant impact on the flow and heat transfer characteristics in thin liquid films over unsteady stretching surfaces.

In recent times, the use of numerical techniques to investigate heat transfer in complex systems has gained momentum. The homotopy analysis method and the finite difference method are among the analytical and numerical methods, respectively, that have received attention due to their ability to approximate solutions for nonlinear problems in various heat transfer scenarios. The homotopy analysis method has been successfully applied in solving a wide range of heat transfer problems [2] [5] [7] [8]. The finite difference method is a popular numerical technique used to solve partial differential equations [3].

Moreover, the study of Lie symmetry has become increasingly significant in recent years as it provides useful insights into the structure and properties of differential equations [4]. In this thesis, Lie symmetry method is utilized to analyze the symmetries in the governing equations, and optimal systems are generated for the obtained Lie symmetries. These optimal systems are employed to obtain the optimal solutions for the heat transfer problem.

1.2 Problem Statement

This heat transfer problem under magnetic field and viscous dissipation has practical applications in several fields, including chemical reactors, biomedical devices, and heat exchangers. Accurately predicting the heat transfer behavior in such systems is a challenging task, and finding optimal solutions for various design and operational parameters is necessary.

To address this challenge, this thesis aims to analyze the heat transfer behavior in a liquid film that is stretched in an unsteady manner while also taking in account the effects of magnetic field and viscous dissipation, incorporating Lie symmetry and optimal systems. The research utilized various analytical and numerical techniques, including the homotopy analysis method and finite difference method, to investigate the problem. To ensure the credibility and precision of the results, they were verified and compared against existing literature.

The main aim of this investigation is to determine the temperature, velocity, and concentration distributions in the liquid film and provide a comprehensive analysis of the

heat transfer characteristics. The outcomes of this research are expected to contribute significantly to the development and enhancement of heat transfer systems through design and optimization for various industrial and biomedical applications.

1.3 Objectives, Scope, and Limitations of the Study

The main objectives of this thesis are:

- To examine the heat transfer characteristics in a liquid film that is flowing over an unsteady stretching surface, considering factors such as viscous dissipation and the presence of an external magnetic field.
- To analyze the symmetries of the governing equations and generate the optimal systems for Lie symmetries.
- To obtain the temperature, velocity, and concentration distributions in the liquid film using homotopy analysis method and finite difference method.
- To validate the findings by comparing them with relevant results in existing literature.

The research questions that will be addressed in this thesis are:

- How do the presence of an external magnetic field and viscous dissipation affect heat transfer in a liquid film that is flowing over an unsteady stretching surface?
- How do Lie symmetry and the optimal systems obtained from Lie symmetry transformations affect the heat transfer solutions?
- What are the profiles of temperature, velocity, and concentration in a liquid film flowing over an unsteady stretching surface, considering the presence of viscous dissipation and an external magnetic field, and how do these profiles compare with those found in existing literature?
- How effective are the homotopy analysis method and finite difference method in solving the heat transfer problems?

The research will be limited to exploring the use of Lie symmetry method to generate optimal systems and applying homotopy analysis method and finite difference method to determine the temperature, velocity, and concentration distributions in the liquid film. By concentrating on these areas, this study aims to provide a comprehensive analysis of the

heat transfer behavior in this system, which can have important implications for designing and optimizing heat transfer systems in various industrial and biomedical applications.

Chapter 2. Literature Review

2.1 Heat Transfer in a Liquid Film over a Moving Surface:

This research topic has practical applications in a variety of industrial processes such as surface cooling, drying of thin sheets, crystal growth, and polymer processing. The significance of this area of study lies in its potential to optimize heat transfer systems and enhance their efficiency, as well as to improve the understanding of complex heat transfer phenomena in practical applications [5]. The unsteady stretching surface enhances the heat transfer rate by creating a thin film that facilitates the transfer of heat and momentum between the fluid and the solid surface [6].

Viscous dissipation and magnetic field are two important factors that affect heat transfer [7]. Viscous dissipation occurs due to the friction between the fluid layers and results in the transfer of energy from the fluid to the surrounding environment [8]. The external magnetic field, on the other hand, can alter the fluid flow patterns and heat transfer characteristics by modifying the fluid properties such as thermal conductivity and viscosity [8].

Several analytical and numerical techniques have been proposed to examine the heat transfer properties of a liquid film flowing over an unsteady stretching surface. Some of the commonly used methods include finite difference method (FDM), homotopy analysis method (HAM), along with Lie symmetry analysis (LSA) [8].

The primary objective of this research is to analyze the heat transfer properties of a liquid film that is flowing over an unsteady stretching surface while being subjected to the effects of viscous dissipation and an external magnetic field. To accomplish this, we employ two numerical techniques, the homotopy analysis method and finite difference method. Furthermore, we will analyze the symmetries of the governing equations using Lie symmetry method and generate optimal systems based on the transformations obtained. By comparing the solutions obtained from these methods and the optimal systems, we provide a comprehensive understanding of heat transfer in this system.

2.2 Influence of Viscous Dissipation on Heat Transfer

Viscous dissipation is a phenomenon in which energy is dissipated in a fluid due to the friction between its layers and the conversion of mechanical energy into heat. In unsteady flow regimes, the overall rate of heat transfer in a liquid film can be significantly affected by this factor.

One of the earliest studies in this area is conducted in [10] where a boundary layer analysis is conducted to examine the effect of viscous dissipation on heat transfer in a liquid film flowing over a stretching surface. The study revealed that the presence of viscous dissipation has a considerable impact on both the rate of heat transfer and the distribution of fluid temperature within the film.

Recent studies have utilized numerical techniques to examine the influence of viscous dissipation on heat transfer in a liquid film that is flowing over an unsteady stretching surface. For example, [11] conducted a study using finite difference method (FDM) to explore the impact of viscous dissipation on heat transfer in a liquid film flowing over a stretching surface. The combined effects of thermal radiation and chemical reaction are also considered in this investigation. The researchers noted that the addition of viscous dissipation has a significant impact on both the rate of heat transfer and the distribution of fluid temperature within the film.

Similarly, [12] have investigated the impact of viscous dissipation on heat transfer in a liquid film over an unsteady stretching surface using different numerical and analytical methods. For instance, researchers utilized a finite volume method to explore the effects of viscous dissipation on heat transfer in a liquid film over a stretching surface with an external magnetic field. Their findings revealed that the inclusion of viscous dissipation results in a considerable enhancement of the heat transfer rate and the fluid temperature distribution in the film. Similarly, in another work a finite difference method is employed to examine the influence of viscous dissipation on the heat transfer characteristics of a liquid film flowing over a stretching surface in the presence of thermal radiation and chemical reaction [5]. They observed that viscous dissipation had a considerable impact on the heat transfer rate and the fluid temperature distribution in the film. In conclusion, the

literature suggests that viscous dissipation plays a crucial role in heat transfer in a liquid film over an unsteady stretching surface.

2.3 Influence of the External Magnetic Field on Heat Transfer

The existence of a magnetic field was found to induce modifications in the flow behavior, the rate of heat transfer, and the thermal stability of the liquid film. Researchers have used various analytical and numerical methods to investigate these effects, including the finite difference method, finite volume method, and boundary element method. The findings of these investigations have demonstrated that the heat transfer properties of the liquid film are affected by the presence of an external magnetic field. In the study [13], they analyzed the magnetic field impact on the hydromagnetic boundary layer flow and heat transfer of the liquid film. The findings of the study showed that the external magnetic field played an important role in enhancing the heat transfer rate and reducing the skin friction coefficient compared to the case without a magnetic field. These results emphasize the importance of considering the external magnetic field when studying heat transfer phenomena occurring in a liquid film flowing over a surface undergoing unsteady stretching. Further research is needed to explore the underlying mechanisms and potential applications of the magnetic field's influence on heat transfer in such systems.

In another study [14], the impact of a transverse magnetic field on heat transfer in a liquid film over an unsteady stretching surface has been analyzed. The study revealed that the introduction of an external magnetic field led to an increase in the heat transfer rate and a decrease in the temperature gradient within the liquid film. The study further reported that the intensity of the magnetic field is directly proportional to the heat transfer rate. Therefore, it is concluded that the presence of an external magnetic field affects the heat transfer characteristics of a liquid film.

Moreover, a study [7], is conducted to analyze the combined effect of magnetic field and viscous dissipation on the heat transfer characteristics of a liquid film over an unsteady stretching surface. The results demonstrated that the magnetic field and viscous dissipation play a crucial role in determining the heat transfer and stability of the liquid film. The inclusion of a magnetic field drastically increased the heat transfer rate and reduced the thermal instability of the liquid film compared to the non-magnetic case. The study also

found that viscous dissipation has a considerable effect on the heat transfer rate, and its inclusion led to a further increase in the heat transfer rate. These findings highlight the importance of considering the combined effects of magnetic field and viscous dissipation on heat transfer in a liquid film over unsteady an stretching surface.

2.4 Symmetry Analysis of Heat Transfer Problems

The Lie symmetry method is a well-established technique for generating optimal systems for a multiple range of mathematical and physical problems. The method has been applied to multiple areas of science, including heat transfer and fluid dynamics.

A Lie symmetry transformation for a system of partial differential equations maintains the structure of the equations. These transformations, known as Lie symmetries, are a useful tool for analyzing the properties of the system. One of the key advantages of the Lie symmetry method is that it allows us to simplify the governing equations, making it easier to find solutions. In particular, the method can be used to reduce the number of independent variables in the system, making it easier to solve the equations numerically or analytically.

The Lie symmetry method is an effective approach for analyzing heat transfer problems by considering the equations that govern the flow of heat in a given system. A notable example of the Lie symmetry method's application is in analyzing the heat transfer in a liquid film over an unsteady stretching surface. The governing equations for this problem include factors such as temperature, velocity, and the impact of external magnetic fields. By using the Lie symmetry method to identify conservation laws and first integrals of the system, the equations' order can be reduced, leading to the discovery of exact solutions. This knowledge can then be applied to optimize heat transfer devices and processes, leading to improved efficiency and sustainability [15].

Once the governing equations have been formulated for a heat transfer problem, the Lie symmetry method can be applied to simplify the system, identify conservation laws, and obtain exact solutions. This approach can be particularly useful in understanding the behavior of heat transfer in a liquid film over an unsteady stretching surface. By finding the Lie symmetries of the system, it is possible to simplify the governing equations, find

conservation laws, and find exact solutions, making it easier to understand and analyze the behavior of the system [16].

2.5 Effectiveness of the Homotopy Analysis Method and Finite Difference Method in Solving Heat Transfer Problems

The application of mathematical methods to solve complex heat transfer problems has been a key area of research in recent years. Two such methods that have been widely used in the field of heat transfer are the Homotopy Analysis Method (HAM) and the Finite Difference Method (FDM).

HAM is an analytical approach that is well-suited to solving nonlinear differential equations. It is a perturbation technique that allows construction of approximate solutions for complex problems that may not be solvable by traditional methods. This methodology has been successfully employed in solving numerous heat transfer problems, exhibiting high accuracy in its solutions [2] [3] [5].

FDM is a numerical technique employed to solve differential equations by dividing the solution domain into a finite number of points. It is a widely used method in the field of heat transfer and has been shown to produce accurate results for a variety of problems.

The effects for the various factors stated earlier are studied using both HAM and FDM. These methods have been successful in producing accurate solutions to these complex problems and have helped in furthering our understanding of heat transfer in such systems.

In summary, the utilization of both HAM and FDM in tackling heat transfer issues has been a critical research focus, resulting in noteworthy progress in comprehending these intricate systems. The use of these numerical techniques has enabled researchers to gain valuable insights into the behavior of such systems, providing a deeper understanding of the underlying physical phenomena and the ability to predict and optimize the heat transfer process. Furthermore, the application of these methods has also led to the development of new techniques for the analysis and optimization of various engineering applications involving heat transfer, such as in the design of heat exchangers and cooling systems.

2.6 Recent Advances in Heat Transfer Analysis for Liquid Films over Unsteady Stretching Surfaces with Magnetic Fields and Viscous Dissipation

There has been an increasing amount of research in recent years that investigates this scenario. These studies have focused on examining different parameters, such as the stretching rate, magnetic field strength, and fluid properties, to gain a better understanding of how they affect the heat transfer behavior of the liquid film.

For example, a study by [13] used numerical simulations to examine the effects. The researchers discovered that the introduction of a magnetic field resulted in an enhancement of the heat transfer rate, while the impact of viscous dissipation became increasingly noticeable as the stretching rate increased.

Another study [16], the researchers used HAM to analyze the heat transfer behavior of a liquid film over an unsteady stretching surface with viscous dissipation and magnetic field. The researchers noted that HAM produced more precise solutions compared to conventional numerical methods. Additionally, they observed that the presence of a magnetic field resulted in an elevated heat transfer rate, particularly at high stretching rates.

In yet another study [15], used the finite difference method (FDM) to examine the effects. The authors found that the FDM provided a more efficient solution compared to multiple scales method, and that the addition of a magnetic field led to an increase in the heat transfer rate, especially at low stretching rates [17].

The Lie symmetry technique can provide analytical solutions that are invariant and transform the system of PDEs into a set of ODEs. This simplifies the mathematical analysis, making the problem more manageable. In my research, I applied this method to explore the heat transfer in a thin liquid film on an unsteady stretching sheet. Specifically, I investigated how parameters such as viscous dissipation and magnetic fields affect the heat transfer. Additionally, I examined the effect of magnetic parameter and viscous dissipation on the velocity and temperature profiles of the thin film flow.

Similarity transformations have been found to be effective in mapping the system of boundary layer equations PDEs with three independent and three dependent terms into a

system of coupled non-linear ODEs with two dependent and one independent variable. However, the similarity transformations remain the same in all of these studies and do not align with the trends observed in real flows [19]. Similarity transformations are invertible transformations of the dependent and independent variables which transformation equations into equations and solutions into solutions.

The Lie symmetry approach has been used to study symmetries of spatial motion of an ideal incompressible shallow water fluid on a rotating plane. However, this approach is limited to the case where Lie point symmetries exist for the differential equations. Numerical methods, such as the shooting and RK4 methods, have been used to solve these problems, but these methods are computationally expensive and may not be able to provide accurate results. Spectral methods have also been used to obtain the solution of these sets of transformed ODEs, but these methods are numerically expensive to compute.

In recent studies, researchers have attempted to solve this type of problem by using central difference with the block elimination method. However, these studies have a limitation on the unsteadiness parameter S. The limit of unsteadiness parameter S is $(S < 2)$ for Newtonian Fluids. The reductions obtained by these studies provide solution for this range of unsteadiness parameter S but the results do not align with the behavior of real accelerating fluids [20].

As a result, there is a need for a new approach that overcomes the limitations of existing methods. The current research proposes the development of a new approach to solve the problem of unsteady boundary layer flow and thin film flow by using Lie symmetry methods to generate optimal systems and using new similarity transformations to generate solutions. The proposed approach will be able to provide a more accurate and comprehensive solution to this problem, considering the limitations of previous methods and aligning with the trends observed in real flows.

In my thesis, I will delve deeper into this field and explore new possibilities. Chapter 3 covers the mathematical formulation of the problem. Chapter 4 focuses on the construction of Lie symmetry transformations. In chapter 5, solution methods for the reduced system of ODEs are presented along with, their validation, and comparison. Chapter 6 presents the similarity solutions for fluid and heat transfer in an unsteady boundary layer flow in the

presence of magnetic parameter. Chapter 7 will present the similarity solutions for unsteady fluid flow and heat transfer in a thin film in the presence of magnetic parameter.

Chapter 3. Mathematical Modelling

In the present research, two different flow conditions are considered. In the coming sections of this chapter, mathematical modelling of each type of flow is discussed.

Mathematical modeling plays a crucial role in understanding the underlying mechanisms and dynamics of heat transfer in a liquid film over an unsteady stretching surface. The governing equations provide a framework for describing the behavior of the system and enable the prediction of the system response to various physical and geometric parameters.

The governing equations for heat transfer in a liquid film over an unsteady stretching surface include the energy equation, the continuity equation, and the boundary conditions. The energy equation describes the conservation of energy in the system. The continuity equation describes the conservation of mass in the system. The boundary conditions specify the conditions at the interface between the liquid film and the unsteady stretching surface. These conditions are usually expressed in terms of temperature, heat flux, and velocity, and they can be either Dirichlet, Neumann, or Robin type.

3.1 Unsteady Fluid Flow and Heat Transfer in Boundary Layer with External Magnetic Field and Viscous Dissipation

The present study mathematically explains the dynamics of a viscous, laminar fluid flow over a horizontal surface subject to unsteady conditions, with the added influence of an external magnetic field and viscous dissipation. The fluid under consideration is assumed to be incompressible, with negligible temperature variations that would affect its viscosity. While gravitational and pressure effects are disregarded in the analysis. The initial conditions for the fluid flow are specified in terms of the velocity and temperature functions as a function of the x-coordinate and time. The surface of the fluid film is presumed to be devoid of any surface waves, and streamwise diffusion is deemed to be insignificant.

Under these assumptions, the governing 2-dimensional boundary layer equations can be expressed mathematically. The Navier-Stokes equation for x-velocity considers the effect of both the external magnetic field and viscous dissipation. The system presenting the fluid flow is expressed as:

Continuity equation:

$$\frac{\partial u}{\partial x} + \frac{\partial v}{\partial y} = 0$$

Navier-Stokes equation for x-velocity:

$$\frac{\partial u}{\partial t} + u\frac{\partial u}{\partial x} + v\frac{\partial u}{\partial y} - \nu\left(\frac{\partial^2 u}{\partial y^2}\right) + \frac{\sigma B^2}{\rho}u = 0$$

Energy equation:

$$\frac{\partial T}{\partial t} + u\frac{\partial T}{\partial x} + v\frac{\partial T}{\partial y} - \frac{\kappa}{\rho Cp}\left(\frac{\partial^2 T}{\partial y^2}\right) - \frac{\mu}{\rho Cp}\left(\frac{\partial u}{\partial y}\right)^2 = 0 \quad (3.1)$$

3.2 The Boundary Conditions

In the mathematical model of a laminar fluid flow, the boundaries of the system are defined through a set of boundary conditions. These conditions provide the information necessary to fully define the solution of the mathematical model and are determined through a combination of physical considerations and mathematical simplicity. In this section, the boundary conditions for the current system will be derived.

The first set of boundary conditions are defined at the surface of the fluid, where $y = 0$. At this location, the velocity components in the x and y directions are given by $u = U(x,t)$ and $v = 0$, respectively. The temperature of the fluid at the surface is also defined as $T = T_s(x,t)$. These conditions describe the velocity and temperature at the surface of the fluid, considering the influence of the external velocity field, $U(x,t)$, and the surface temperature, $T_s(x,t)$. The second set of boundary conditions are defined at the free surface of the fluid, where $y = h(t)$ because this function determines the location of the boundary between the fluid and the surrounding environment. By specifying the boundary conditions in terms of this function, we can ensure that the velocity and temperature of the fluid are properly defined at the interface between the fluid and the surrounding medium. At this location, the y-component of the velocity is set to zero, i.e., $\frac{\partial u}{\partial y} = 0$, to ensure that there is no normal flow at the surface. Additionally, the temperature derivative in the y direction is also set to zero, i.e., $\frac{\partial T}{\partial y} = 0$, to ensure that the temperature does not change in the normal

direction. Finally, the velocity in the y direction is defined as $v = \frac{\partial h}{\partial t}$, which represents the velocity of the free surface.

In conclusion, the boundary conditions for the mathematical model of a laminar fluid flow include conditions at the surface of the fluid and the free surface. These conditions ensure that the solution of the mathematical model is physically meaningful and consistent with the underlying physics of the problem.

The boundary conditions for this mathematical model can be summarized as follows:

At $y = 0$ (the thin film surface), the following conditions hold:

a. $u = U(x,t)$

b. $v = 0$

c. $T = T_s(x,t)$

At $y = h(t)$ (the upper boundary), the following conditions hold:

d. $\frac{\partial u}{\partial y} = 0$

e. $\frac{\partial T}{\partial y} = 0$

f. $v = \frac{\partial h}{\partial t}$ (3.2)

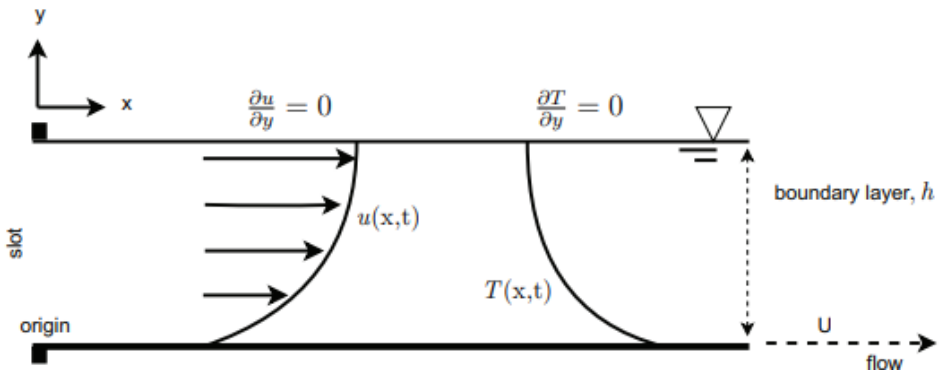

Figure 3.1: Diagram illustrating fluid flow and heat transfer over an unsteady stretching surface

Chapter 4. Lie Symmetries and Invariants

The research explores the movement of fluid in a liquid film that experiences viscous dissipation and an external magnetic field. The motion of the fluid is due to the stretching of the sheet in a specific direction. The velocity and temperature of the sheet are considered to be positive constants, denoted as α, b, and ν, where ν represents the kinematic viscosity, and the temperature at the slit and the reference temperature are represented by T_0 and T_s, respectively.

$$U(x,t) = \frac{bx}{1-\alpha t}, \qquad T_s(x,t) = T_0 - T_{ref}\left(\frac{bx^2}{2\nu(1\ -\ \alpha t)^{\frac{3}{2}}}\right) \tag{4.1}$$

The use of these particular forms for the velocity, temperature, and magnetic field enables the construction of similarity transformations, which is a crucial aspect of this study.

$$B(x,t) = \frac{B_0}{\sqrt{1\ -\ \alpha t}} \tag{4.2}$$

To simplify the analysis of fluid flow and heat transfer, we apply similarity transformations to the partial differential equations (3.1) that describe the flow. Through this method, the governing equations can be simplified from having three dependent and three independent variables to a system of ordinary differential equations.

$$y\ =\ 0, \qquad u = U(x,t), \qquad v\ =\ 0, \qquad T = T_s(x,t),$$

$$y\ =\ h(t),\ u_y = T_y = 0,\ v\ =\ h_t = \frac{dh}{dt}\,, \tag{4.3}$$

A similarity transformation

$$f(\eta) = \frac{\psi(x,y,t)}{x\sqrt{\frac{b\nu}{1\ -\ \alpha t}}}, \qquad \theta\ (\eta) = \frac{T_0 - T(x,y,t)}{T_{ref}\left(\frac{bx^2}{2\nu}\right)(1\ -\ \alpha t)^{\frac{3}{2}}}, \qquad \eta\ = \frac{y}{\beta}\sqrt{\frac{b}{\nu(1\ -\ \alpha t)}} \tag{4.4}$$

is constructed through the stream function,

$$u = \frac{\partial \psi}{\partial y} = \frac{bx}{1 - \alpha t} f', \qquad v = -\frac{\partial \psi}{\partial x} = -\beta \sqrt{\frac{b\nu}{1 - \alpha t}}\, f \tag{4.5}$$

There transformations map the boundary layer equations to following system of ODEs:

$$f''' + \gamma f'^2 + \gamma \left(\frac{S\eta}{2} - f\right) f'' + \gamma (S - Mn) f' = 0$$
$$Pr^{-1}\, \theta'' + 2\gamma (S + f')\theta + \gamma \left(\frac{S\eta}{2} - f\right) \theta' + Ecf''^2 = 0 \tag{4.6}$$

and conditions

$$f(0) = 0, \qquad f'(0) = 1, \qquad \theta\,(0) = 1,$$

$$f(1) = \frac{S}{2}, \qquad f''(1) = 0, \qquad \theta'(1) = 0 \tag{4.7}$$

The system of PDEs is subject to certain conditions, including the film thickness denoted by $h(t)$, which is a function of the similarity variable η, with prime denoting the derivative with respect to η. The magnetic parameter Mn and the Eckert number Ec are defined, respectively, as $\frac{\sigma B_0^2}{b\rho}$ and $\frac{U^2}{C_p T_s - T_0}$. The Prandtl number, Pr, is given by $\frac{(\nu \rho C_p)}{\kappa}$, while β is a constant found by the HAM. Moreover, β is dimensionless and represents the film thickness at the free surface. Finally, S is defined as $\frac{\alpha}{b}$ that shows unsteadiness, and we obtain $h(t) = \beta \sqrt{\frac{\nu(1-\alpha t)}{b}}$ at the free surface.

To obtain new similarity transformations for the system of partial differential equations related to my thesis topic, the first step is to derive Lie point symmetry generators. This involves finding the infinitesimal generator $\boldsymbol{X}$ of the Lie symmetry group for the system of partial differential equations. The generator $\boldsymbol{X}$ represents the directional flow of the symmetry transformations and helps in finding invariant solutions and simplifying the original system of partial differential equations. A symmetry generator for (3.1) reads as

$$\boldsymbol{X} = \xi_k \frac{\partial}{\partial \psi_k} + \phi_k \frac{\partial}{\partial \zeta_k}, \tag{4.8}$$

The infinitesimal coordinates ξ_k and ϕ_k are functions of the independent variables x, y, t, and the dependent variables u, v, and T, represented by $k = 1, 2, 3$.

Due to the presence of first and second-order partial derivatives in the system of equations (3.1) and associated boundary conditions (3.2), necessitates to employ the first and second-order extensions of the Lie point symmetry generators. $\boldsymbol{X}^{[1]}$ denotes the first-order extension, whereas $\boldsymbol{X}^{[2]}$ represents the second-order extension.

To demonstrate the extension technique, the second order extension can be represented as

$$\boldsymbol{X}^{[2]} = \boldsymbol{X}^{[1]} + \phi_k^t \frac{\partial}{\partial \zeta_{k,t}} + \phi_k^x \frac{\partial}{\partial \zeta_{k,x}} + \phi_k^y \frac{\partial}{\partial \zeta_{k,y}} + \phi_k^{tt} \frac{\partial}{\partial \zeta_{k,tt}} + \phi_k^{xx} \frac{\partial}{\partial \zeta_{k,xx}} + \phi_k^{yy} \frac{\partial}{\partial \zeta_{k,yy}} \tag{4.9}$$

This is an equation that represents the form of a second-order differential operator, known as the Lie derivative along a one-parameter Lie group of transformations. The operator is defined by a vector field $\boldsymbol{X}$ and acts on the dependent variables of a partial differential equation (PDE) system. The coefficients ϕ_k^t, ϕ_k^x, ϕ_k^y, ϕ_k^{tt}, ϕ_k^{xx}, and ϕ_k^{yy} are functions of the independent variables, dependent variables, and their partial derivatives.

The extension coefficients are obtained through the following formulas.

$$\phi_k^n = D_n \phi_k - \zeta_{k,t} D_n(\xi_1) - \zeta_{k,x} D_n(\xi_2) - \zeta_{k,y} D_n(\xi_3) \tag{4.10}$$

where $n \in \{t, x, y\}$ and $k = 1, 2, 3$.

$$\Phi_k^{tt} = D_t \phi_k^t - \zeta_{k,tt} D_t(\xi_1) - \zeta_{k,tx} D_t(\xi_2) - \zeta_{k,ty} D_t(\xi_3).$$

$$\Phi_k^{xx} = D_x \phi_k^x - \zeta_{k,tx} D_x(\xi_1) - \zeta_{k,xx} D_x(\xi_2) - \zeta_{k,xy} D_x(\xi_3).$$

$$\Phi_k^{yy} = D_y \phi_k^y - \zeta_{k,ty} D_y(\xi_1) - \zeta_{k,yx} D_y(\xi_2) - \zeta_{k,yy} D_y(\xi_3). \tag{4.11}$$

where

$$D_n = \frac{\partial}{\partial n} + \zeta_{k,n} \frac{\partial}{\partial k} + \zeta_{k,nn} \frac{\partial}{\partial k, n} + \ldots, \tag{4.12}$$

To find the infinitesimal coordinates, ξ_k and ψ_k, of the operator in equation (4.8), a second order extension, $\boldsymbol{X}^{[2]}$, is applied to the system of partial differential equations (PDEs) in equation (3.1). One specific PDE in this system, the continuity equation, is used to explain an invariance criterion, that is

$$\boldsymbol{X}^{[2]}\left(\frac{\partial u}{\partial x}+\frac{\partial v}{\partial y}\right)\Big|_{\frac{\partial u}{\partial x}+\frac{\partial v}{\partial y}=0}=0 \tag{4.13}$$

The LHS of the equation evaluates the action of the generator $\boldsymbol{X}^{[2]}$ on the incompressibility condition, and the RHS is equal to zero, meaning that the action of $\boldsymbol{X}^{[2]}$ preserves the incompressibility of the fluid flow. Solving the PDE given by such invariance criterion of all equations in system (3.1) yields the following symmetries:

Table 4.1: Lie Symmetries

Symmetry	***Generator***
$\boldsymbol{X}_1$	$\frac{\partial}{\partial x}$
$\boldsymbol{X}_2$	$\frac{\partial}{\partial T}$
$\boldsymbol{X}_3$	$x\frac{\partial}{\partial x}+u\frac{\partial}{\partial u}+2T\frac{\partial}{\partial T}$
$\boldsymbol{X}_4$	$t\frac{\partial}{\partial t}+\frac{y}{2}\frac{\partial}{\partial y}-u\frac{\partial}{\partial u}-\frac{v}{2}\frac{\partial}{\partial v}-2T\frac{\partial}{\partial T}$
$\boldsymbol{X}_5$	$t^{1-\frac{\sigma B_0^2}{\rho\alpha^2}}\frac{\partial}{\partial x}+\frac{\rho\alpha^2-\sigma Bo^2}{\rho\alpha^2 t}t^{1-\frac{\sigma B_0^2}{\rho\alpha^2}}\frac{\partial}{\partial u}$

In order to ensure the validity of Lie solutions to the system of PDEs (3.1), it is necessary to consider the invariance of associated boundary conditions (3.2) as well. It is important that these conditions remain invariant under the symmetry generators $\boldsymbol{X}_1$, $\boldsymbol{X}_2$, ..., $\boldsymbol{X}_7$. Typically, when applying a single symmetry generator to the boundary conditions, both U and T become functions of either x or t. However, in this study, it is desired to keep them as functions of both x and t. To achieve this, linear combinations of the symmetry generators $\boldsymbol{X}_1$, $\boldsymbol{X}_2$, ..., $\boldsymbol{X}_7$ are formed by adding two at a time. The resulting combinations,

shown in Table 4.2, ensure that the boundary conditions (3.2) remain invariant while allowing for U and T to remain functions of both space and time. This is a crucial aspect of the research, as it ensures that the solutions obtained are physically meaningful and applicable to the specific problem at hand.

The study employs Lie point symmetries to investigate the similarity solutions of the system of PDEs (3.1). This involves applying the infinitesimal generator $\boldsymbol{X}$ on the PDE system and equating the resulting expression to zero, leading to a system of PDEs that involve the infinitesimal coordinates ξ_k and ϕ_k and their partial derivatives. By solving these PDEs, the Lie point symmetries of the system are obtained. However, to ensure that these symmetries also yield similarity solutions, they must satisfy the boundary conditions (3.2) as well. To achieve this, linear combinations of the symmetry generators are used, which, when applied to the boundary conditions, give rise to linear PDEs and solving them invariance of the boundary conditions of the type (3.2) is achieved.

Table 4.2: Symmetries and Invariants

Case	**Symmetry**	**Invariants**
1	$\boldsymbol{X}_3 + \alpha \boldsymbol{X}_4$	$tx^{-\alpha}, yx^{-\frac{\alpha}{2}}, ux^{\alpha-1}, vx^{\frac{\alpha}{2}}, x^{2(\alpha-1)}T$
2	$\boldsymbol{X}_4 + \alpha \boldsymbol{X}_1$	$te^{-\frac{x}{\alpha}}, ye^{-\frac{x}{2\alpha}}, ue^{\frac{x}{\alpha}}, ve^{\frac{x}{2\alpha}}, Te^{\frac{2x}{\alpha}}$
3	$\boldsymbol{X}_3$	$t, y, \frac{u}{x}, v, \frac{T}{x^2}$

Chapter 5. Numerical and Analytical Solution Methods

HAM allows for the deformation of a given problem into a simpler one, which is particularly useful for solving non-linear problems where traditional methods may not be applicable. The Homotopy Analysis Method has been widely applied in various fields, including fluid dynamics and heat transfer.

In addition to the HAM, this research also employs the FDM as a numerical solution technique. The FDM is a popular method for solving differential equations, especially those that are difficult or impossible to solve analytically. This involves the discretization of differential equations into a system of algebraic equations, which are subsequently solved numerically. This method is widely applicable and can be employed to solve a variety of problems, even those involving complex geometries and boundary conditions.

Finally, in this research in-house codes are developed with MAPLE, that is a powerful tool for symbolic mathematical computations. MAPLE is widely used in scientific and engineering research, and it is particularly useful for solving mathematical problems that involve symbolic manipulation. In-house codes developed using MAPLE are highly efficient and can be tailored specifically to the problem at hand, providing a level of flexibility and precision.

Overall, the combination of these three approaches allows a comprehensive and detailed exploration of the mathematical structures of the problem at hand, providing a deeper understanding of the underlying physics of unsteady boundary layer flow and thin film flow in the presence of a magnetic field. The results obtained from these methods are compared and evaluated to determine the most effective solution technique for this type of problem.

We assumed that a set of base functions, η_m, where m ranges from 0 to 15, could express the solution of $f(\eta)$ and $\theta(\eta)$. To obtain the solution, we used the boundary conditions (4.8) to express the initial functions $f_0(\eta)$ and $\theta_0(\eta)$ as follows:

$$f_0(\eta) = \eta + 3\frac{(S-2)}{4}\,\eta^2 - \frac{(S-2)}{4}\eta^3, \qquad \theta_0(\eta) = 1 \tag{5.1}$$

To make the tedious procedure of HAM, which is presented in various research papers such as [1] and [11], easy to program, we used a different approach. We expanded each variable in the system (4.7) as follows:

$$F = \sum_{m=0}^{n} q^m f_m(\eta) = q^0 f_0(\eta) + q^1 f_1(\eta) + \ldots + q^n f_n(\eta)$$

$$F' = \sum_{m=0}^{n} q^m f'_m(\eta) = q^0 f'_0(\eta) + q^1 f'_1(\eta) + \ldots + q^n f'_n(\eta) \tag{5.2}$$

Similarly,

$$F'' = \sum_{m=0}^{n} q^m f''_m(\eta), \qquad F''' = \sum_{m=0}^{n} q^m f'''_m(\eta), \qquad g = \sum_{m=0}^{n} q^m \gamma_m(\eta)$$

$$\theta = \sum_{m=0}^{n} q^m \theta_m(\eta), \qquad \theta' = \sum_{m=0}^{n} q^m \theta'_m(\eta), \qquad \theta'' = \sum_{m=0}^{n} q^m \theta''_m(\eta) \tag{5.3}$$

The final form becomes,

$$\begin{aligned} &\sum_{m=0}^{n} q^m f'''_m(\eta) \\ &\quad + \sum_{m=0}^{n} q^m \gamma_m(\eta) \left(\left(\sum_{m=0}^{n} q^m f'_m(\eta) \right)^2 \right. \\ &\quad \left. + \left(\frac{S\eta}{2} - \sum_{m=0}^{n} q^m f_m(\eta) \right) \sum_{m=0}^{n} q^m f''_m(\eta) + (S - Mn) \sum_{m=0}^{n} q^m f'_m(\eta) \right) \\ &\quad = 0 \end{aligned}$$

$$Pr^{-1}\sum_{m=0}^{n} q^m \theta''_m(\eta) + \sum_{m=0}^{n} q^m \gamma_m(\eta)\left(2\left(S+\sum_{m=0}^{n} q^m f'_m(\eta)\right)\sum_{m=0}^{n} q^m \theta_m(\eta) + \left(\frac{S\eta}{2}-\sum_{m=0}^{n} q^m f_m(\eta)\right)\sum_{m=0}^{n} q^m \theta'_m(\eta)\right) + Ec\left(\sum_{m=0}^{n} q^m f''_m(\eta)\right)^2 = 0 \quad (5.4)$$

The present study aims to find analytical solutions for a specific set of boundary conditions by using the method outlined by Wang [1]. The first step is to write the boundary conditions in the form of

$$f_m(0) = 0, f'_m(0) = 0, \theta_m(0) = 0,$$

$$f_m(1) = 0, f''_m(1) = 0, \theta'_m(1) = 0 \quad (5.5)$$

To find the particular solutions we use the following:

$$f^*_m(\eta) = \iiint_0^{\eta} h_f H_f f^*_n(\eta) d\eta d\eta d\eta$$

$$\theta^*_m(\eta) = \iint_0^{\eta} h_\theta H_\theta \theta^*_n(\eta)\, d\eta d\eta \quad (5.6)$$

The parameters h_f and h_θ are non-zero auxiliary parameters that control the convergence of the solution, and $H_f(\eta)$ and $H_\theta(\eta)$ are non-zero auxiliary functions that are typically equal to 1. The general solution is then given by

$$f_m(\eta) = \bar{f}^*_m(\eta) + a_1 + a_2\eta + a_3\eta^2$$

$$\theta_m(\eta) = \bar{\theta}^*_m(\eta) + a_4 + a_5\eta, \quad (5.7)$$

where $a_1, a_2, a_3, a_4\ and\ a_5$ are constants

$$f(\eta) \approx \sum_{m=0}^{n} f_m(\eta) \quad (5.8)$$

$$\theta(\eta) \approx \sum_{m=0}^{n} \theta_m(\eta) \tag{5.9}$$

$$g \approx \sum_{m=0}^{n} g_m \tag{5.10}$$

In the present study, the symbolic mathematical tool MAPLE is used to construct the 15^{th} order approximate solutions.

Chapter 6. Similarity Transformations and Double Reductions of the Flow Model

Similarity transformations are introduced here and their importance in reducing the complexity of the Navier-Stokes equations is illustrated. The various steps involved in constructing similarity transformations are then discussed in detail, with a focus on identifying the relevant scaling parameters and ensuring that the transformed equations satisfy the necessary physical and mathematical requirements.

Construction of similarity transformations is based on the concept of double reductions, which yields simplification of the transformed equations by reducing them to a set of ODEs. The chapter presents various examples to illustrate the use of these techniques and concludes with a discussion of their advantages, limitations, and future research directions. In summary, this chapter provides a comprehensive guide for utilizing similarity transformations and double reductions as powerful tools in reducing the complexity of the Navier-Stokes equations for numerical simulations of fluid flow.

Table 6.1: Symmetries

Case	Symmetry	Invariants
1	$\boldsymbol{X}_3 + \alpha \boldsymbol{X}_4, \alpha \neq 0$	$tx^{-\alpha}, yx^{-\frac{\alpha}{2}}, ux^{\alpha-1}, vx^{\frac{\alpha}{2}}, x^{2(\alpha-1)}T$
2	$\boldsymbol{X}_3$	$t, y, \frac{u}{x}, v, \frac{T}{x^2}$
3	$\boldsymbol{X}_4 + a\boldsymbol{X}_1, \alpha \neq 0$	$te^{-\frac{x}{a}}, ye^{-\frac{x}{2a}}, ue^{\frac{x}{a}}, ve^{\frac{x}{2a}}, Te^{\frac{2x}{a}}$
General	$C_1\boldsymbol{X}_1 + C_2\boldsymbol{X}_2 + C_3\boldsymbol{X}_3 + C_4\boldsymbol{X}_4$	$t, y, \frac{u}{x}, v, \frac{T}{x^2}$

6.1 Case 1

The first reduction involved the use of Lie symmetry to simplify the system of partial differential equations. By finding the invariance that leaves both $u_y = 0$ and $T_y = 0$, we extended the generator and derived a PDE which led to the calculation of invariants. These

invariants were then used as new independent and dependent variables in the system, which was then mapped to a simpler form for easier solving using the similarity method.

$$(1-a)G + az_1 G_{z_1} - \frac{a}{2} z_2 G_{z_2} + H_{z_2} = 0$$

$$G_{z_1} + (1-a)G^2 - az_1 G G_{z_1} - \frac{a}{2} z_2 G G_{z_2} + H G_{z_2} - \nu \mathrm{G}_{z_2,z_2} + \frac{\sigma B_o^2}{\alpha^2 \rho z_1} G = 0$$

$$K_{z_1} + 2(1-a)GK - az_1 G K_{z_1} - \frac{a}{2} z_2 G K_{z_2} + H K_{z_2} - \frac{\kappa}{\rho C_p} \mathrm{K}_{z_2,z_2} - \frac{\omega}{\rho C_p} G_{z_2}^2 = 0 \qquad (6.1)$$

Subjected to boundary conditions

$$z_2 = 0, \qquad H = 0, \qquad G = U(z_1), \qquad K = T_s(z_1)$$

$$z_2 = c_1\sqrt{z_1}, \qquad H = \frac{c_1}{2\sqrt{z_1}}, \qquad G_{z_2} = 0, \qquad K_{z_2} = 0 \qquad (6.2)$$

Admitted symmetry

Symmetry is an important concept in mathematics, and we can use it to simplify complex systems of equations. In this step, we identified a certain symmetry in the system of partial differential equations that we are studying. This symmetry allows us to find new variables that satisfy the system and its conditions.

$$y = \mathrm{z}_1 \partial \mathrm{z}_1 + \frac{\mathrm{z}_2}{2} \partial_{z_2} - G\, \partial_G - \frac{H}{2} \partial_{\mathrm{H}} - 2k\, \partial_k \qquad (6.3)$$

Invariants $\left\{ \frac{\mathrm{z}_2}{\sqrt{z_1,}}, \mathrm{z}_1 G, \sqrt{z_1} H, z_1^2 K \right\}$

This gave us new variables

$$w = \frac{z_2}{\sqrt{z_1}}, P = z_1 G, Q = \sqrt{z_1} H, R = z_1^2 K \qquad (6.4)$$

Second reduction

In this step, we further simplified the system of partial differential equations by applying a second reduction. This involved finding new equations that satisfy the system and its

conditions, and introducing new variables that helped us solve the system using the similarity method.

$$P + Q_w = 0$$

$$vP_{w,w} - \left(Q - \frac{w}{2}\right)P_w - P^2 + \left(1 - \frac{\sigma B_o^2}{\alpha^2 \rho}\right)P = 0$$

$$2R(P-1) + \left(Q - \frac{w}{2}\right)R_w - \frac{\kappa}{\rho C_\varphi}R_{\mathrm{w,w}} - \frac{\omega}{\rho c_p}P_w^2 = 0 \tag{6.5}$$

Subject to the conditions

$$\begin{aligned} w = 0, \quad Q = 0, \quad P = c_1, \quad R = c_2 \\ w = c_3, \quad Q = \frac{c_3}{2}, \quad P_w = 0, \quad R_w = 0. \end{aligned} \tag{6.6}$$

Similarity transformation

In this step, we used a similarity transformation to map the system of PDEs to a simpler form. This allows us to solve the system using certain invariants, which we identified by introducing new variables and applying certain boundary conditions. The resulting system is easier to solve using numerical methods or other techniques.

The reduced system of ODEs derived here includes the quantities Pr, S, Ec and Mn to satisfy the system and its conditions.

$$\beta\sqrt{\frac{\alpha v}{b}}\eta = w \; -\frac{b}{\alpha}f' = \mathrm{P},\; \beta\sqrt{\frac{vb}{\alpha}}f = \mathrm{Q},\; \theta = \mathrm{R} \tag{6.7}$$

Through this process, an invertible similarity transformation is obtained.

$$y = \beta\sqrt{\frac{\alpha v t}{b}}\eta,\; u = -\frac{bx}{\alpha t}f',\; v = \beta\sqrt{\frac{vb}{\alpha t}}f,\; T = \frac{x^2}{t^2}\theta \tag{6.8}$$

This transformation maps the system to the following system of ODEs

$$f''' + \gamma f'^2 + \gamma\left(\frac{S\eta}{2} - f\right)f'' + \gamma(S - Mn)f' = 0$$

$$Pr^{-1}\,\theta'' + 2\gamma(S + f')\theta + \gamma\left(\frac{S\eta}{2} - f\right)\theta' + Ecf''^2 = 0 \qquad (6.9)$$

6.2 Case 2

The first reduction

$$G + H_{z_2} = 0$$

$$G_{z_1} + \mathrm{H}G_{z_2} + \mathrm{G}^2 - \nu\mathrm{G}_{z_2,z_2} + \frac{\sigma B_0^2}{\alpha^2\rho z_1}G = 0$$

$$K_{z_1} + 2\mathrm{GK} + HK_{z_2} - \frac{\kappa}{\rho\varphi}\mathrm{K}_{z_2,z_2} - \frac{\omega}{\rho C_p}G_{z_2}^2 = 0 \qquad (6.10)$$

Subjected to boundary conditions

$$z_2 = 0, \qquad G = U(z_1), \qquad H = 0, \qquad K = T_s(z_1)$$

$$z_2 = h(z_1), \qquad G_{z_2} = 0, \qquad K_{z_2} = 0, \qquad H = \frac{dh}{dz_1} \qquad (6.11)$$

Admitted symmetry

$$y = z_1\partial z_1 + \frac{z_2}{2}\partial z_2 - G\partial_G - \frac{H}{2}\partial_H - 2K\partial_K \qquad (6.12)$$

Invariants $\left\{\frac{\mathrm{z}_2}{\sqrt{z_1}}, \mathrm{z}_1 G, \sqrt{z_1}H, z_1^2 K\right\}$

This gave us new variables

$$w = \frac{z_2}{\sqrt{z_1}}, P = z_1 G, Q = \sqrt{z_1}H, R = z_1^2 K \qquad (6.13)$$

Second reduction

$$P + Q_w = 0$$

$$vP_{w,w} - \left(Q - \frac{w}{2}\right)P_w - P^2 + \left(1 - \frac{\sigma B_o^2}{\alpha^2\rho}\right)P = 0$$

$$2R(P - 1) + \left(Q - \frac{w}{2}\right)R_w - \frac{\kappa}{\rho C_\varphi}R_{w,w} - \frac{\omega}{\rho c_p}P_w^2 = 0 \qquad (6.14)$$

Subject to the conditions

$$w = 0, \qquad Q = 0, \qquad P = c_1, \qquad R = c_2$$

$$w = c_3, \qquad Q = \frac{c_3}{2}, \qquad P_w = 0, \qquad R_w = 0. \tag{6.15}$$

Similarity transformation

The reduced system of ODEs derived here includes the quantities Pr, S, Ec and Mn to satisfy the system and its conditions.

$$\beta\sqrt{\frac{\alpha v}{b}}\eta = w \; -\frac{b}{\alpha}f' = \mathrm{P},\; \beta\sqrt{\frac{vb}{\alpha}}f = \mathrm{Q},\; \theta = \mathrm{R} \tag{6.16}$$

Through this process, an invertible similarity transformation is obtained.

$$y = \beta\sqrt{\frac{\alpha v t}{b}}\eta,\; u = -\frac{bx}{\alpha t}f',\; v = \beta\sqrt{\frac{vb}{\alpha t}}f,\; T = \frac{x^2}{t^2}\theta \tag{6.17}$$

This transformation maps the system to the following system of ODEs

$$\begin{aligned} &f''' + \gamma f'^2 + \gamma\left(\frac{S\eta}{2} - f\right)f'' + \gamma(S - Mn)f' = 0 \\ &Pr^{-1}\,\theta'' + 2\gamma(S + f')\theta + \gamma\left(\frac{S\eta}{2} - f\right)\theta' + Ecf''^2 = 0. \end{aligned} \tag{6.18}$$

6.3 Case 3

The first reduction

$$\begin{aligned} &H_{z_2} - \frac{1}{a}\left(G + z_1 G_{z_1} + z_2 G_{z_2}\right) = 0 \\ &G_{z_1} - \frac{1}{a}\left(G + z_1 G_{z_1} + z_2 G_{z_2}\right) + HG_{z_2} - \nu \mathrm{G}_{z_2,z_2} + \frac{\sigma B_o^2}{\alpha^2 \rho z_1}G = 0 \\ &K_{z_1} - \frac{1}{a}G\left(2K + z_1 K_{z_1} + \frac{z_2}{2}K_{z_2}\right) + HK_{z_2} - \frac{\kappa}{\rho C_p}K_{z_2,z_2} - \frac{\omega}{\rho C_p}G_{z_2}^2 = 0 \end{aligned} \tag{6.19}$$

Subjected to boundary conditions

$$z_2 = 0, \qquad G = U(z_1), \qquad H = 0, \qquad G_{z_2} = 0$$

$$z_2 = c\sqrt{z_1}, \qquad H = \frac{c}{2\sqrt{z_1}}, \qquad K = T_s(z_1), \qquad K_{z_2} = 0 \tag{6.20}$$

Admitted symmetry

$$y = z_1\partial z_2 + \partial_H \tag{6.21}$$

Invariants $\left\{\mathrm{z}_1, \sqrt{\mathrm{G}}, (1 - \frac{z_2}{Z_1})H, K\right\}$

This gave us new variables

$$w = z_1, P = \sqrt{G}, Q = \left(1 - \frac{z_2}{Z_1}\right)H, R = K \tag{6.22}$$

Second reduction

$$\begin{aligned} &P + wP_w = 0 \\ &P_w - \frac{1}{\alpha}(P + wP_w) + \frac{\sigma B_0^2}{\alpha^2\rho\omega}P = 0 \\ &R_w - \frac{1}{2}P(2R + wR_w) = 0 \end{aligned} \tag{6.23}$$

Subject to the conditions

$$w = 0, \qquad Q = 0, \qquad P = c_1, \qquad R = c_2$$

$$w = c_3, \qquad Q = \frac{c_3}{2}, \qquad P_w = 0, \qquad R_w = 0. \tag{6.24}$$

This system does not need to be transformed as the Q term is seen to be eliminated and this does not lead to a system of ODE's with a third order ODE. This is the type of case which is over-constrained which is why it is not solved here.

6.4 General Case

The first reduction

$$\begin{aligned} &G_{z_1} + H_{z_2} = 0 \\ &-\frac{\mathrm{z}_1 C_3}{C_4}G_{z_1} - \frac{\mathrm{z}_2}{2}G_{z_2} + \mathrm{G}\mathrm{G}_{z_1} + \mathrm{H}G_{z_2} + \frac{\mathrm{C}_3 - \mathrm{C}_4}{C_4}\mathrm{G} - \nu\mathrm{G}_{z_2,z_2} + \frac{\sigma B_0^2}{\alpha^2\rho}G = 0 \\ &-\frac{z_1 C_3}{C_4}K_{z_1} - \frac{\mathrm{z}_2}{2}\mathrm{K}_{z_2} + \frac{(C_3 - C_4)}{C_4}2\mathrm{K} + \mathrm{G}\mathrm{K}_{z_1} + HK_{z_2} - \frac{\kappa}{\rho\varphi}\mathrm{K}_{z_2,z_2} - \frac{\omega}{\rho C_p}G_{z_2}^2 = 0 \end{aligned} \tag{6.25}$$

Subjected to boundary conditions.

$$z_2 = 0, \qquad G = U(z_1), \qquad H = 0, \qquad K = T_s(z_1)$$

$$z_2 = h(z_1), \qquad G_{z_2} = 0, \qquad K_{z_2} = 0, \qquad H = \frac{dh}{dz_1} \tag{6.26}$$

Admitted symmetry

$$y = z_1 \partial z_1 + G\partial_G + 2K\partial_K \tag{6.27}$$

Invariants $\left\{z_2, \frac{G}{z_1}, H, \frac{K}{z_1^2}\right\}$

This gave us new variables

$$w = z_2, P = z_1 G, Q = H, R = z_1^2 K \tag{6.28}$$

Second reduction

$$P + Q_w = 0$$

$$-\frac{C_3}{C_4}P - \frac{w}{2}P_w + \frac{C_3 - C_4}{C_4}P + P^2 + QP_w - vP_{\mathrm{w,w}} + \frac{\sigma B_o^2}{\alpha^2 \rho}P = 0$$

$$-\frac{C_3}{C_4}2R - \frac{w}{2}R_w + \frac{C_3 - C_4}{C_4}2R + 2PR + QR_w - \frac{\kappa}{\rho C_p}R_{w,w} - \frac{\omega}{\rho c_p}P_w^2 = 0 \tag{6.29}$$

This reduction simplifies and eliminates the constants, so we get the same equation we got previously.

$$P + Q_w = 0$$

$$-P - \frac{w}{2}P_w + P^2 + QP_w - vP_{w,w} + \frac{\sigma B_o^2}{\alpha^2 \rho}P = 0$$

$$-2R - \frac{w}{2}R_w + 2PR + QR_w - \frac{\kappa}{\rho C_p}R_{w,w} - \frac{\omega}{\rho c_p}P_w^2 = 0 \tag{6.30}$$

Subject to the conditions

$$w = 0, \quad Q = 0, \quad P = c_1, \quad R = c_2$$
$$w = c_3, \quad Q = \frac{c_3}{2}, \quad P_w = 0, \quad R_w = 0. \tag{6.31}$$

Similarity transformation

The reduced system of ODEs derived here includes the quantities Pr, S, Ec and Mn to satisfy the system and its conditions.

$$\beta\sqrt{\frac{\alpha v}{b}}\eta = w \; -\frac{b}{\alpha}f' = \mathrm{P},\; \beta\sqrt{\frac{vb}{\alpha}}f = \mathrm{Q},\; \theta = \mathrm{R} \tag{6.32}$$

Through this process, an invertible similarity transformation is obtained.

$$y = \beta\sqrt{\frac{\alpha v t}{b}}\eta,\; u = -\frac{bx}{\alpha t}f',\; v = \beta\sqrt{\frac{vb}{\alpha t}}f,\; T = \frac{x^2}{t^2}\theta \tag{6.33}$$

This transformation maps the system to the following system of ODEs

$$f''' + \gamma f'^2 + \gamma\left(\frac{S\eta}{2} - f\right)f'' + \gamma(S - Mn)f' = 0$$
$$Pr^{-1}\,\theta'' + 2\gamma(S + f')\theta + \gamma\left(\frac{S\eta}{2} - f\right)\theta' + Ecf''^2 = 0 \tag{6.34}$$

6.5 Implemented System

The optimal systems and a general case are considered, and similarity transformation are derived. The flow model is reduced using the obtained similarity transformation. For all cases we obtain the following system of ODEs:

Table 6.2: Final Systems

Symmetries	Transformed system
$\boldsymbol{X}_3 + \alpha \boldsymbol{X}_4$	$f''' + \gamma f'^2 + \gamma\left(\frac{S\eta}{2} - f\right) f'' + \gamma(S - Mn) f' = 0$ $\mathrm{Pr}^{-1}\ \theta'' + 2\gamma(S + f')\theta + \gamma\left(\frac{S\eta}{2} - f\right)\theta' + Ecf''^2 = 0.$
$\boldsymbol{X}_3$	$f''' + \gamma f'^2 + \gamma\left(\frac{S\eta}{2} - f\right) f'' + \gamma(S - Mn) f' = 0$ $\mathrm{Pr}^{-1}\ \theta'' + 2\gamma(S + f')\theta + \gamma\left(\frac{S\eta}{2} - f\right)\theta' + Ecf''^2 = 0.$
$C_1\boldsymbol{X}_1 + C_2\boldsymbol{X}_2 + C_3\boldsymbol{X}_3 + C_4\boldsymbol{X}_4$	$f''' + \gamma f'^2 + \gamma\left(\frac{S\eta}{2} - f\right) f'' + \gamma(S - Mn) f' = 0$ $\mathrm{Pr}^{-1}\ \theta'' + 2\gamma(S + f')\theta + \gamma\left(\frac{S\eta}{2} - f\right)\theta' + Ecf''^2 = 0.$

The boundary conditions became:

$$f(0) = 0, \qquad f'(0) = 1, \qquad \theta(0) = 1,$$

$$f(1) = \frac{S}{2}, \qquad f''(1) = 0, \qquad \theta'(1) = 0 \tag{6.35}$$

In Table 7.1 three different cases, namely $\boldsymbol{X}_3 + \alpha \boldsymbol{X}_4, \boldsymbol{X}_3$, and $C_1\boldsymbol{X}_1 + C_2\boldsymbol{X}_2 + C_3\boldsymbol{X}_3 + C_4\boldsymbol{X}_4$, are presented and transformation to final form has been done. Interestingly, the final form of system of reduced ODEs in these cases is found to be the same.

The implemented system is described by two coupled differential equations. The first equation is a third-order differential equation for the temperature distribution, $f(\eta)$, which is a function of the spatial coordinate η. This equation involves terms such as the third derivative of f, f''' and its first and second derivatives, f' and f'', respectively. The equation also includes parameters such as γ, S, Mn, and η.

The second equation is a second-order differential equation for the dimensionless stream function, $\theta(\eta)$, which is also a function of the spatial coordinate η. This equation includes

terms such as the second derivative of θ, θ'', and its first derivative, θ', as well as the first derivative of f, f'. This equation also involves parameters such as γ, S, Mn, η, and Ec.

The implemented system is subject to boundary conditions that determine the values of f and θ at both ends of the channel. These conditions include $f(0) = 0$ and $f'(0) = 1$, which establish a fixed velocity at the lower wall and a stationary wall. Furthermore, the condition $\theta(0) = 1$ sets a fixed temperature at the lower wall. The upper wall is subject to the conditions $f(1) = \frac{S}{2}$, indicating that the velocity at the upper wall is half that of the lower wall, and $f''(1) = 0$, indicating that the pressure gradient at the upper wall is zero. Lastly, the condition $\theta'(1) = 0$ indicates no heat transfer at the upper wall.

Chapter 7. Finite Difference Method

The research presented in this study involves solving a system of nonlinear ordinary differential equations (ODEs) using the method of difference equations. To accomplish this, forward finite differencing schemes are employed to discretize the system of nonlinear ODEs (4.7) into a system of difference equations. The resulting difference equations, along with the given boundary conditions (4.8), are then solved using the Newton-Raphson method. This approach is particularly useful for systems of nonlinear ODEs that cannot be solved analytically or by other numerical methods. To ensure the accuracy of our solutions, we have also implemented finite difference scheme. For this purpose, we have utilized forward difference schemes at $\eta = 0$ and backward difference schemes at $\eta = 1$. The use of these techniques and tools in conjunction allows us to achieve highly accurate solutions for the non-linear system of ODEs under consideration in this study.

Forward difference:

$$\frac{df}{d\eta} = \frac{f(\eta_{i+1}) - f(\eta_i)}{h} \tag{7.1}$$

$$\frac{d^2f}{d\eta^2} = \frac{f(\eta_{i+2}) - 2f(\eta_{i+1}) + f(\eta_i)}{h^2} \tag{7.2}$$

$$\frac{d^3f}{d\eta^3} = \frac{f(\eta_{i+3}) - 3f(\eta_{i+2}) + 3f(\eta_{i+1}) - f(\eta_i)}{h^3} \tag{7.3}$$

Backward difference:

$$\frac{df}{d\eta} = \frac{f(\eta_i) - f(\eta_{i-1})}{h} \tag{7.4}$$

$$\frac{d^2f}{d\eta^2} = \frac{f(\eta_i) - 2f(\eta_{i-1}) + f(\eta_{i-2})}{h^2} \tag{7.5}$$

$$\frac{d^3f}{d\eta^3} = \frac{f(\eta_i) - 3f(\eta_{i-1}) + 3f(\eta_{i-2}) - f(\eta_{i-3})}{h^3} \tag{7.6}$$

The first-order accurate O(h) finite difference approximations for the first, second, and third-order derivatives are used in the process. The resulting non-linear algebraic equations are solved implicitly by iterating the Newton-Raphson method with an initial guess of 0.2

for each term until the error is less than 10^{-10}. The dimensionless film thickness λ is an unknown variable in this system, which is made consistent by using the boundary condition provided in (4.8). The stability of the system is found to be satisfactory during the study.

7.1 Validation of Results

In this research, HAM is utilized to solve a non-linear coupled system of ODEs presented in equation (4.6). The HAM approach is an improvement on the method proposed by Wang [1] as it expands all terms individually rather than simultaneously. The results are validated by comparing them with those of Wang [1] in Table 7.1. The 15^{th} order HAM results show good agreement with Wang's results, with a deviation of less than 0.00007. These results are used as a benchmark for comparison with the Finite Difference Method (FDM) results presented in Table 7.1 and Table 7.2.

7.2 Comparison of Solution Methods

In the current study, Table 7.1 illustrates the impact of unsteadiness parameter S on the film thickness λ and skin friction $f''(0)$ that have been determined using FDM with 2000 nodes, and HAM. It is observed that the HAM solution demonstrates good convergence at higher values of unsteadiness parameter S.

Table 6.2 illustrates the influence of Prandtl number Pr on the surface temperature $\theta(1)$ and heat flux $\theta'(0)$ that have been determined using the finite difference method with 2000 nodes, and Homotopy Analysis Method (HAM). On the other hand, the numerical method, the finite difference method, can compute results for these values of Prandtl number. The comparison of results obtained from these different methods aids in the verification and validation of results obtained by the FDM. The system of non-linear ODEs is solved using Newton's iteration method, and the error between the numerical solution and analytical solution is found to be less than 0.09%. To assess the effectiveness of numerical solution methods in regions where analytical techniques may fail, a comparison is made between the finite difference method and Homotopy Analysis Method. The results obtained from both methods are in good agreement, as shown in Table 7.1.

Table 7.1: Validation of Results

S	FDM		HAM (15th order)		Error
	β	$f''(0)$	β	$f''(0)$	
0.5	4.201564784	−3.733414657	4.200727468	−3.733402849	$8.4 * 10^{-4}$
0.7	2.158612579	−2.718487262	2.157625689	−2.718582938	$9.9 * 10^{-4}$
0.9	1.317561235	−2.033348615	1.317819600	−2.033348467	$2.6 * 10^{-4}$
1	1.065413587	−1.725132059	1.064350595	−1.725132061	$1.0 * 10^{-4}$
1.2	0.715315574	−1.331743214	0.715315670	−1.331730153	$9.6 * 10^{-8}$
1.4	0.481647891	−0.957835792	0.479888132	−0.957826447	$1.8 * 10^{-4}$
1.5	0.384652317	−0.785666542	0.385409030	−0.785657910	$2.4 * 10^{-4}$

Table 7.2: Validation of Results

Pr	FDM		HAM (15th order)		Error
	$\theta(1)$	$\theta'(0)$	$\theta(1)$	$\theta'(0)$	
0.05	1.086787616	0.206263	1.086883256	0.206364	$9.5 * 10^{-5}$
0.06	1.105548321	0.249781	1.105613246	0.249880	$6.5 * 10^{-5}$
0.07	1.124731747	0.294108	1.124830389	0.294208	$9.8 * 10^{-5}$
0.08	1.144491179	0.339473	1.144551882	0.339376	$6.7 * 10^{-5}$
0.09	1.164743819	0.385567	1.164806928	0.385417	$6.3 * 10^{-5}$
0.10	1.185534262	0.432176	1.185602771	0.432363	$6.8 * 10^{-5}$

7.3 Computation Time

Table 7.3: Film thickness λ and skin friction f variation with order of HAM

Order of HAM	**Compute time (sec)**	β	$f''(0)$
2	1.2	0.7144701269	−1.331170826
5	2.3	0.7153168290	−1.331729681
8	3.8	0.7153140585	−1.331730038
10	6.2	0.7153140083	−1.331730006
12	8.4	0.7153137910	−1.331729863
15	12.5	0.7153156700	−1.331730153

The results obtained from the analysis of the order of HAM and computation time for the heat transfer equations are presented in the Table 7.3. The calculations were carried out using a computer with an Intel(R) Core(TM) i7-7700HQ CPU @ 2.80GHz 2.81 GHz and 12 GB RAM. The values of β and $f''(0)$ for different orders of HAM are obtained, and it is observed that the values are consistent across all orders of HAM. As the order of the HAM increases, the computation time also increases, making it a computationally expensive method for higher-order solutions.

According to the findings, as the order of the HAM increased from 2 to 15, the computation time also increased from 1.2 seconds to 12.5 seconds. However, it is important to note that even with an increase in the order of HAM, the values of β and $f''(0)$ remained relatively constant till 4^{th} decimal place, indicating that the solution is stable and reliable.

Overall, the results of this study suggest that a higher order of HAM leads to a more accurate solution, but at the expense of increased computation time. Therefore, the choice of HAM order should be made based on the balance between computational resources and the required accuracy of the solution. These findings are significant in the development of more accurate and efficient numerical methods for solving complex heat transfer equations in various engineering applications.

Chapter 8. Results and Discussion

This section presents key findings of the study and provides a detailed analysis of the results obtained from the methodology described in the previous section. This section presents the results of the similarity transformations and double reductions performed on the Navier-Stokes equations, including the derived reduced system of ODEs. The section then discusses the numerical solutions of the reduced system of ODEs for various values of the scaling parameters and physical properties of the fluid flow. The study results are visually presented in the form of tables and graphs that depict fluid flow patterns and the impact of different physical parameters on flow behavior, providing a comprehensive illustration of the results.

The discussion section then delves deeper into the interpretation of the results, highlighting the key insights gained from the study. The discussion examines the effects of various physical parameters on the fluid flow, including the Prandtl number, and the geometrical characteristics of the flow domain. The section also evaluates the performance of the similarity transformations and double reductions in reducing the complexity of the Navier-Stokes equations and facilitating the numerical simulation of fluid flow. Finally, the section concludes by providing a summary of the findings of the study and their implications for the field of fluid dynamics, as well as suggestions for future research in this area.

Table 8.1: Variation in film thickness β with unsteadiness S and magnetic parameter Mn

Mn	$S = 0.5$	$S = 0.7$	$S = 0.9$	$S = 1.0$	$S = 1.2$	$S = 1.4$	$S = 1.5$
5	4.200727	2.157636	1.317824	1.064351	0.715314	0.479888	0.385409
6	3.330918	1.700584	1.028113	0.824712	0.544815	0.357457	0.283289
7	2.760233	1.403570	0.842920	0.673206	0.439966	0.284801	0.223951
8	2.356749	1.194989	0.714297	0.568748	0.368965	0.236693	0.185165
9	2.039973	1.040425	0.619749	0.492360	0.317699	0.202489	0.157832
10	1.809418	0.921291	0.547313	0.434067	0.278943	0.176923	0.137530

The Table 8.1 shows the film thickness values for different values of magnetic parameter Mn and unsteadiness parameter S. The film thickness is an important parameter that characterizes the behavior of fluid motion within a liquid film. As the value of Mn increases

from 5 to 10, the film thickness decreases for all values of S. This is because an increase in Mn results in a stronger magnetic field, which causes the fluid to become more constrained and flow in a more restricted manner. As a result, the thickness of the liquid film decreases.

Similarly, as the value of S increases from 0.5 to 1.5, the film thickness decreases for all values of Mn. This is because an increase in S indicates that the motion of the sheet becomes more unsteady, which leads to a more turbulent flow of the liquid film. Consequently, the fluid flow is constrained to a smaller region, which leads to a decrease in the thickness of the liquid film.

Overall, the results show that both the magnetic parameter Mn and the unsteadiness parameter S have a significant impact on the behavior of fluid motion within a liquid film. By understanding the relationship between these parameters and the film thickness, the behavior of liquid films in various applications can be controlled.

Table 8.2: Variation in $f'(\eta)$ and $\theta(\eta)$ with S, Mn and Pr

$\boldsymbol{Mn}$	$f'(1)$	$\theta(1)$ $\boldsymbol{Pr = 0.05}$	$\theta(1)$ $\boldsymbol{Pr = 0.06}$	$\theta(1)$ $\boldsymbol{Pr = 0.07}$	$\theta(1)$ $\boldsymbol{Pr = 0.08}$	$\theta(1)$ $\boldsymbol{Pr = 0.09}$	$\theta(1)$ $\boldsymbol{Pr = 0.1}$
$\boldsymbol{S = 0.5}$							
5	0.026523	1.157968	1.193940	1.231595	1.271069	1.312505	1.355506
7.5	0.032626	1.096385	1.117178	1.138560	1.160520	1.183095	1.206315
10	0.034214	1.071482	1.086595	1.101988	1.117675	1.133670	1.149983
$\boldsymbol{S = 1.0}$							
5	0.282537	1.086885	1.105613	1.124829	1.144553	1.164803	1.185600
7.5	0.285033	1.052393	1.063332	1.074434	1.085700	1.097135	1.108741
10	0.286042	1.038826	1.046831	1.054918	1.063090	1.071346	1.079690
$\boldsymbol{S = 1.5}$							
5	0.629464	1.046026	1.055634	1.065383	1.075275	1.085315	1.095504
7.5	0.630354	1.024864	1.029950	1.035074	1.040237	1.045440	1.050682
10	0.630669	1.017481	1.021032	1.024601	1.028187	1.031792	1.035416

The Table 8.2 displays the impact of varying the magnetic parameter Mn and unsteadiness parameter S on the heat and mass transfer characteristics of thin film flows over stretching sheets. Moreover, it presents temperature distribution for different Prandtl number Pr. Results indicate that as Mn increases, the velocity gradient f' of the fluid also increases due to the magnetic field generated by the sheet, resulting in enhanced heat transfer θ. Conversely, increasing S leads to a decrease in f' and θ due to reduced fluid movement and contact with the sheet. Higher Pr values lead to a decreased θ because thicker thermal boundary layers reduce heat transfer rates. These findings demonstrate the significant effects of magnetic and unsteadiness parameters on the heat transfer characteristics of thin film flows over stretching sheets, which can be manipulated by adjusting these parameters.

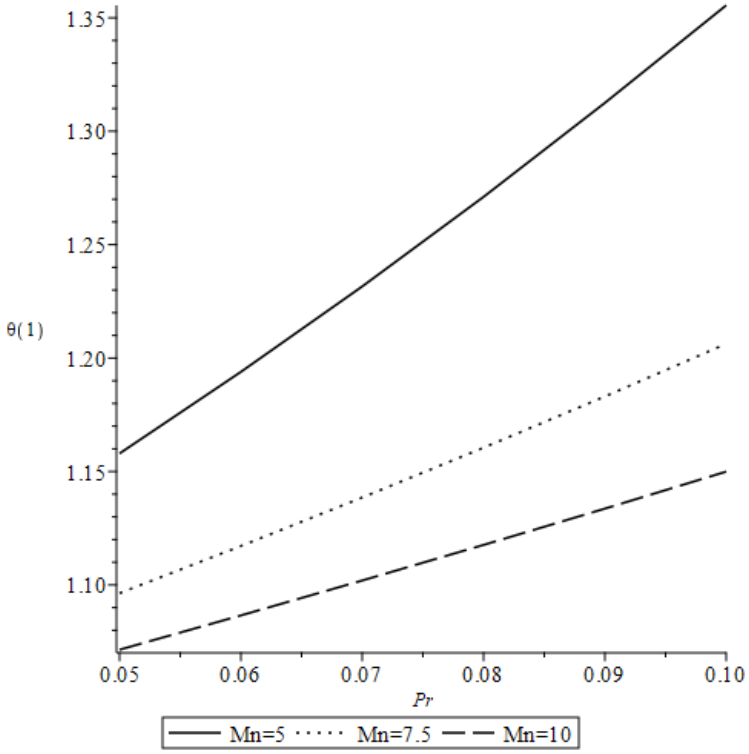

Figure 8.1: Variation of $\theta(1)$ with Pr as $S = 0.5$

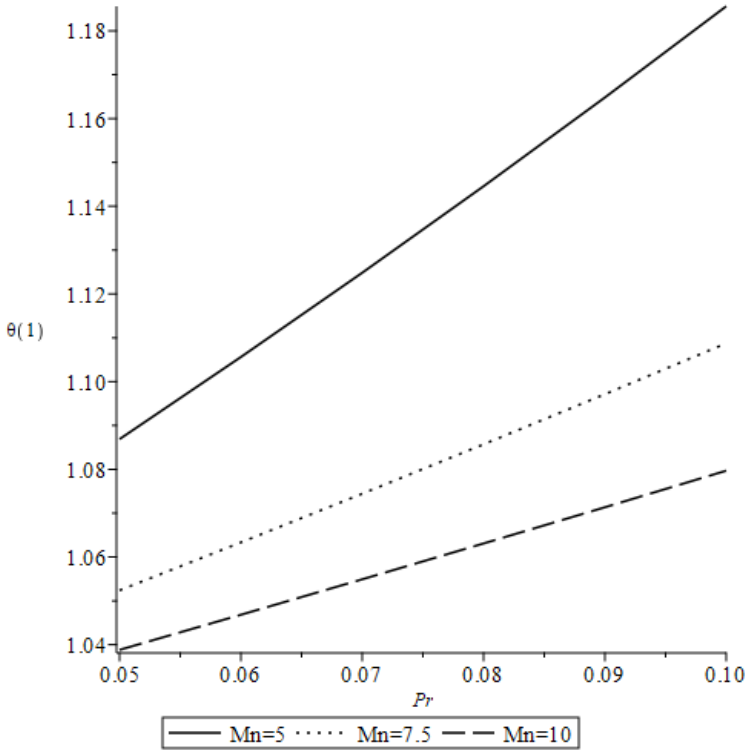

Figure 8.2: Variation of $\theta(1)$ with Pr as $S = 1.0$

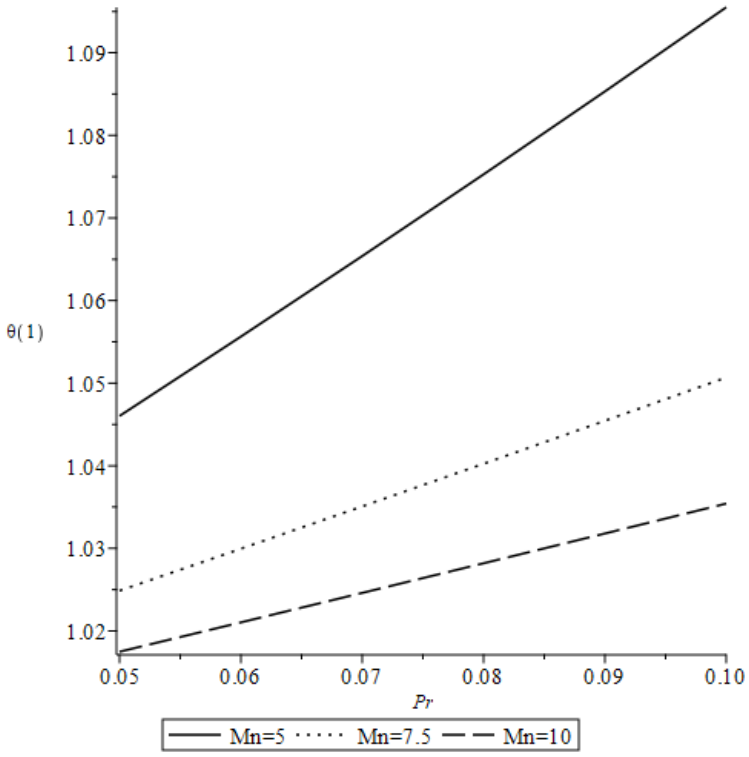

Figure 8.3: Variation of $\theta(1)$ with Pr as $S = 1.5$

The plots of θ with a variation of Pr, indicating that the temperature distribution follows a predictable pattern as the Prandtl number increases. However, the slope of the curve varies depending on the value of Mn. As Mn increases from 5 to 10, the slope of the curve becomes less steep, indicating a decrease in the rate of change of temperature with respect to the Prandtl number. This suggests that the magnetic field has a stabilizing effect on the temperature distribution in the flow, reducing the sensitivity of the temperature to changes in the Prandtl number. The steepness of the curve for $Mn = 5$ compared to the other values further emphasizes this trend. These results have important implications for the design and optimization of magnetic fields in industrial processes involving fluid flow and can develop more efficient and sustainable technologies.

Table 8.3: Variation in $f'(\eta)$ and $\theta(\eta)$ with S, Mn and Pr for $S = 0.5$

$\boldsymbol{Ec}$	$f'(1)$	$\theta(1)$ $\boldsymbol{Pr = 0.05}$	$\theta(1)$ $\boldsymbol{Pr = 0.06}$	$\theta(1)$ $\boldsymbol{Pr = 0.07}$	$\theta(1)$ $\boldsymbol{Pr = 0.08}$	$\theta(1)$ $\boldsymbol{Pr = 0.09}$	$\theta(1)$ $\boldsymbol{Pr = 0.1}$
$\boldsymbol{Mn = 5}$							
1	0.026523	1.157968	1.193940	1.231595	1.271069	1.312505	1.355506
3	0.026523	1.186461	1.229036	1.273689	1.320542	1.369785	1.421655
5	0.026523	1.215068	1.264189	1.315801	1.370025	1.427070	1.487212
$\boldsymbol{Mn = 7.5}$							
1	0.032626	1.096385	1.117178	1.138560	1.160520	1.183095	1.206315
3	0.032626	1.123065	1.149694	1.177085	1.205256	1.234238	1.264075
5	0.032626	1.149740	1.182198	1.215610	1.249987	1.285378	1.321834
$\boldsymbol{Mn = 10}$							
1	0.034214	1.071482	1.086595	1.101988	1.117675	1.133670	1.149983
3	0.034214	1.097523	1.118149	1.139200	1.160679	1.182592	1.204958
5	0.034214	1.123410	1.149688	1.176407	1.203679	1.231512	1.259933

Table 8.4: Variation in $f'(\eta)$ and $\theta(\eta)$ with S, Mn and Pr for $S = 1.5$

$\boldsymbol{Ec}$	$f'(1)$	$\theta(1)$ $\boldsymbol{Pr = 0.05}$	$\theta(1)$ $\boldsymbol{Pr = 0.06}$	$\theta(1)$ $\boldsymbol{Pr = 0.07}$	$\theta(1)$ $\boldsymbol{Pr = 0.08}$	$\theta(1)$ $\boldsymbol{Pr = 0.09}$	$\theta(1)$ $\boldsymbol{Pr = 0.1}$
$\boldsymbol{Mn = 5}$							
1	0.629464	1.046026	1.055634	1.065383	1.075275	1.085315	1.095504
3	0.629464	1.050679	1.061263	1.072002	1.082903	1.093967	1.105198
5	0.629464	1.055332	1.066890	1.078622	1.090531	1.102619	1.114891
$\boldsymbol{Mn = 7.5}$							
1	0.630354	1.024864	1.029950	1.035074	1.040237	1.045440	1.050682
3	0.630354	1.029386	1.035398	1.041457	1.047563	1.053716	1.059917
5	0.630354	1.033904	1.040845	1.047840	1.054888	1.061992	1.069152
$\boldsymbol{Mn = 10}$							
1	0.630669	1.017481	1.021032	1.024601	1.028187	1.031792	1.035416
3	0.630669	1.021958	1.026418	1.030902	1.035409	1.039940	1.044495
5	0.630669	1.026433	1.031804	1.037203	1.042631	1.048088	1.053575

To provide a more accurate explanation of the above tables, it shows the values of the temperature distribution parameter θ for different values of Eckert number Ec and dimensionless velocity f' for various values of Prandtl number Pr ranging from 0.05 to 0.1.

The table indicates that there is no significant effect of Eckert number on the dimensionless velocity f'. The value of f' remains constant at 0.026523 for all the values of Ec, suggesting that the velocity of the fluid is not affected by the Eckert number due to the non-existence of this number in the velocity equations that is not coupled with the second equation.

However, the results indicate that the values of θ increase as the Eckert number increases. This implies that the Eckert number has a considerable effect on the temperature distribution in the fluid. As the Eckert number increases, the fluid's energy increases, resulting in a more uniform temperature distribution. This trend is observed for all values of Pr. All these results are shown in Table 8.3 and Table 8.4.

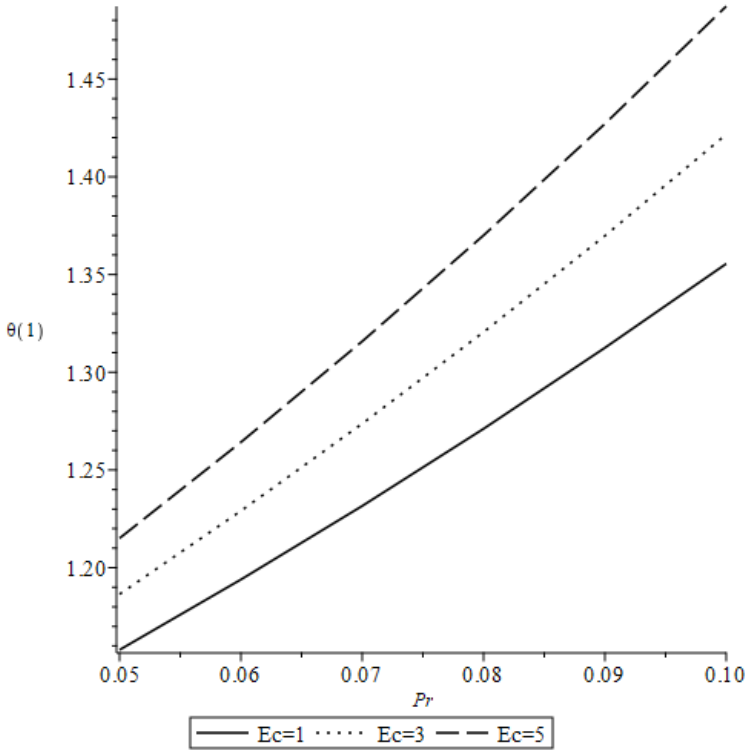

Figure 8.4: Variation of $\theta(1)$ with Pr as $Mn = 5$

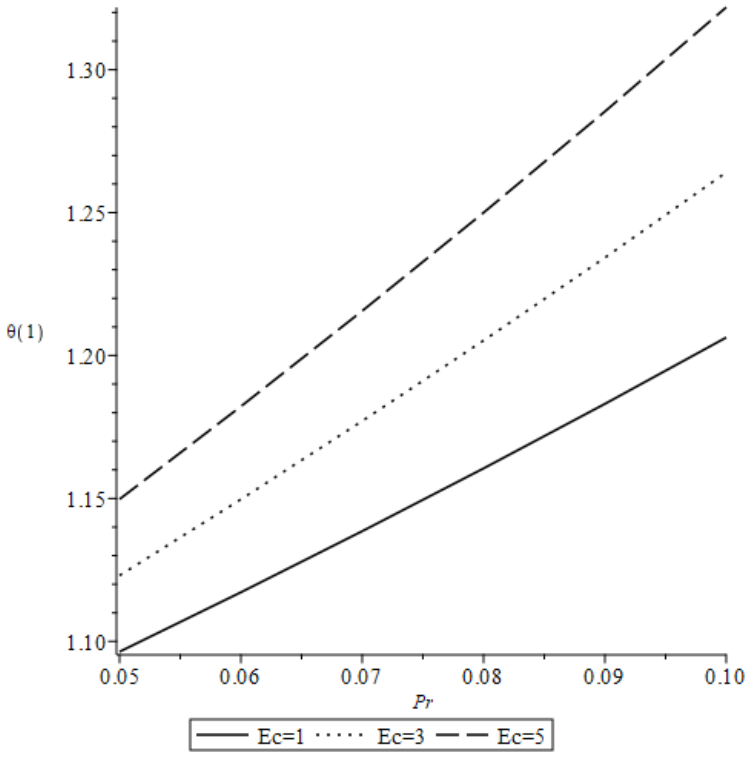

Figure 8.5: Variation of $\theta(1)$ with Pr as $Mn = 7.5$

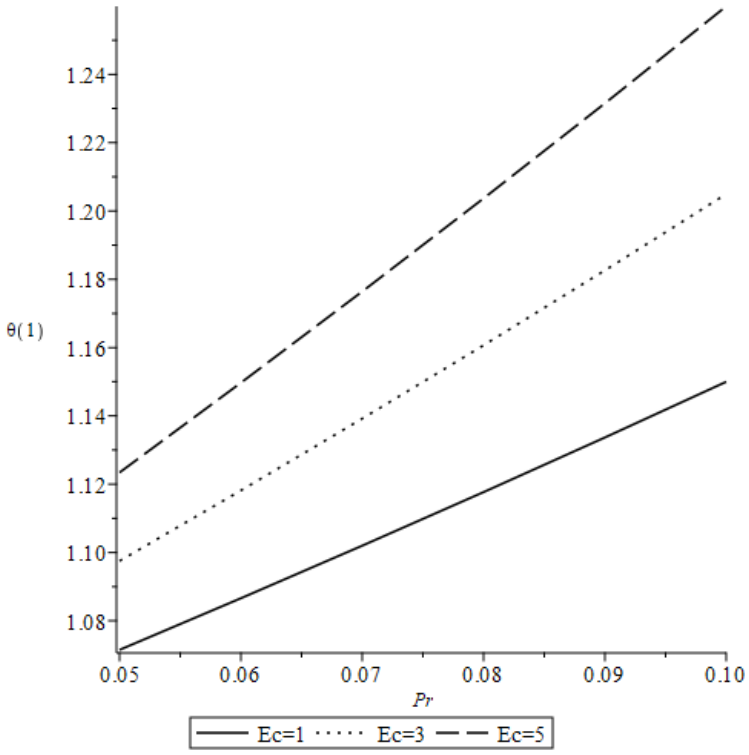

Figure 8.6: Variation of $\theta(1)$ with Pr as $Mn = 10$

The temperature distribution plots for various Ecket numbers Ec and Prandtl numbers Pr indicate a direct linear relationship between temperature and Pr number. The temperature increases with increasing Pr number for all Ec values. The plots for different Ec values demonstrate that as the value of Ec increases, the slope of the curve also increases, implying that the magnetic field has a more significant effect on temperature distribution. Notably, the $Ec = 5$ curve has a steeper slope than the other two curves, implying that a more potent magnetic field can cause a more significant change in the temperature distribution. However, these findings align with the anticipated behavior of fluid flow under the influence of a magnetic field, where the field can induce convective motion and change the temperature distribution in the fluid. Overall, these results offer insight into the intricate relationship between magnetic fields, fluid flow, and temperature distribution in practical engineering systems.

8.1 Effect of Unsteadiness on the Boundary Layer Thickness and Fluid Velocity

Table 8.5: Effect of Unsteadiness on β and f' for $Mn = 5$, $Ec = 1$

S	h_1	β	$f'(1)$	$f''(0)$
0.5	-0.1	4.200727468	0.02651777121	-3.733402849
1	-0.8	1.064350595	0.2777140390	-1.725132061
1.5	-1	0.385409030	0.6294643239	-0.7856579100
2.5	-1	-0.4861298706	1.375217221	0.7473965361
3	-1	-2.550489381	1.725959701	1.684306489
4	-1	0.9839147941	2.579359123	2.434904615
5	-1	0.5155264233	3.352517940	3.760291470

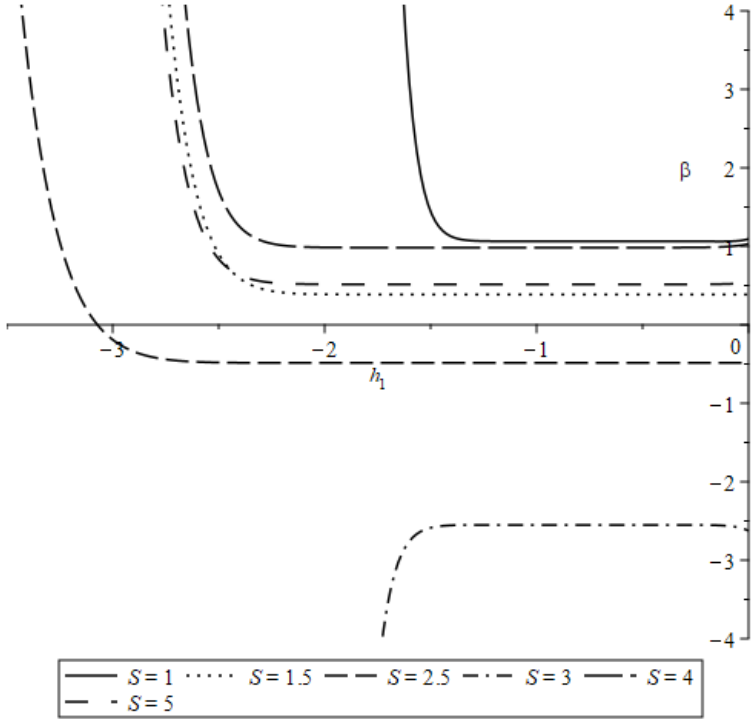

Figure 8.7: h_1-curve

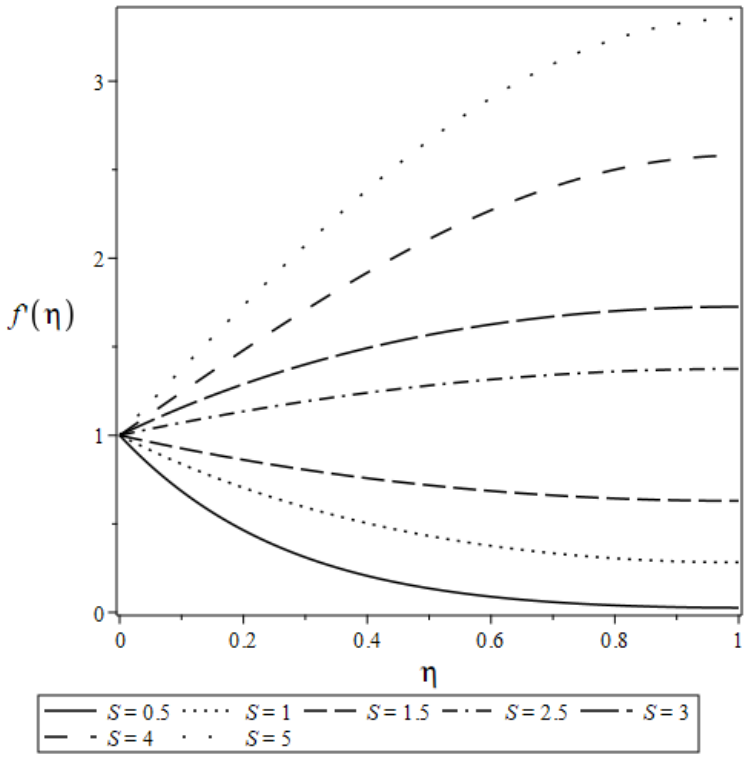

Figure 8.8: f' Variation for different S values

The outcomes of the current investigation reveal that the heat transfer properties are significantly influenced by the homotopy parameter, the unsteadiness parameter, and the film thickness. The homotopy parameter, denoted by h_1, is employed in the homotopy analysis technique to convert the original nonlinear differential equation into a series of deformation equations that can be solved analytically. The negative values of h_1 in this research imply that the homotopy parameter has an impact on the equation's solution, and its magnitude decreases as the stretching parameter, S, increases. The negative values of the film thickness, represented by β, indicate that the liquid film free surface is located below the stretching plate surface, indicating the presence of dry patches on the plate surface. To ensure a continuous and smooth liquid film over the plate, the value of the unsteadiness parameter should be selected within a certain range. In the present study, the negative values of β were observed when the unsteadiness parameter was 2.5 and 3. Further ahead the for the unsteadiness values 4 and 5, the film thickness is again positive. Due to the discontinuity at 2.5 and 3, it is recommended to select the range of the unsteadiness parameter from 0.5 to 1.5 to ensure a continuous liquid film over the plate.

These findings are of significant importance for understanding the behavior of fluids in various industrial and natural processes, such as heat exchangers, coatings, and boundary layer flows.

It is important to note that $f'(1)$ should be below 1 to ensure a stable lubrication film. This is because the value of $f'(1)$ represents the slope of the lubrication film at the exit, and if it is greater than 1, the film thickness will decrease rapidly, leading to a breakdown of the lubrication film. Therefore, to maintain a stable lubrication film, it is crucial to keep the value of $f'(1)$ below 1.

8.2 Effect of Unsteadiness on Temperature

Table 8.6: Variation with S for $Mn = 5$, $Ec = 1$ and $h_2 = -0.06$

$\boldsymbol{S}$	$\theta(1)$	$\theta'(0)$
0.5	1.157957115	0.437771
0.7	1.119649013	0.309671
0.9	1.096379966	0.234875
1	1.086883256	0.206364
1.2	1.069898690	0.158651
1.4	1.053985374	0.117841
1.5	1.046025366	0.098710

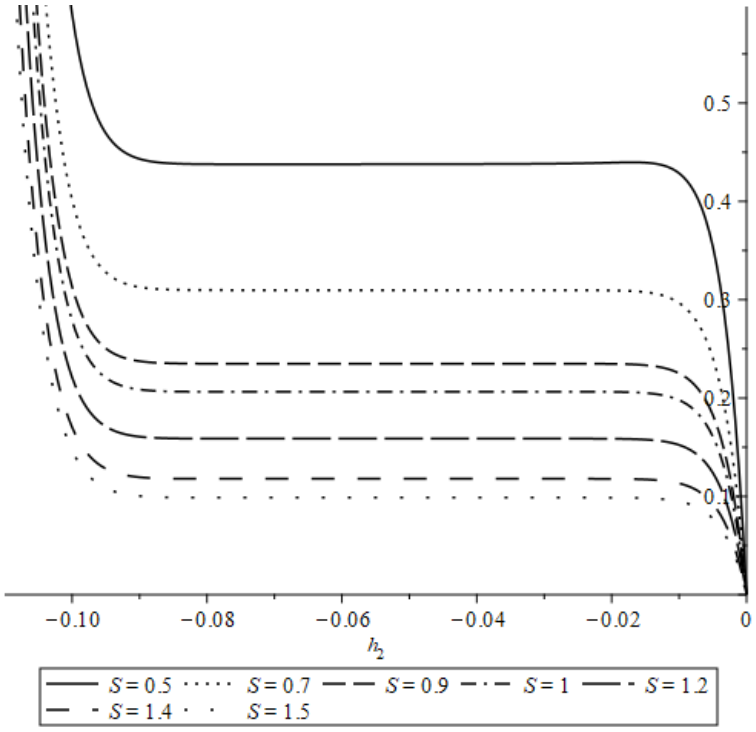

Figure 8.9: h_2-curve

The h_2 curves are plotted for the system to study the effect of unsteadiness on the temperature distribution. The stability range is seen to be constant for increasing values of S, which indicates that the system remains stable under the influence of unsteadiness. However, the value of $\theta'(0)$ decreases with increasing S, which indicates that the temperature gradient near the surface of the film is reduced due to unsteadiness.

This is because the unsteadiness of the system introduces temporal variations in the temperature distribution of the fluid, leading to reduced temperature gradients near the surface of the film. As a result, the heat transfer rate from the film to the surrounding fluid decreases, leading to a reduction in the overall heat transfer rate. The impact of this reduction in temperature gradient near the film surface on the design and heat transfer cannot be ignored. Therefore, it is crucial to account for the effect of unsteadiness on temperature distribution to ensure accurate prediction of heat transfer.

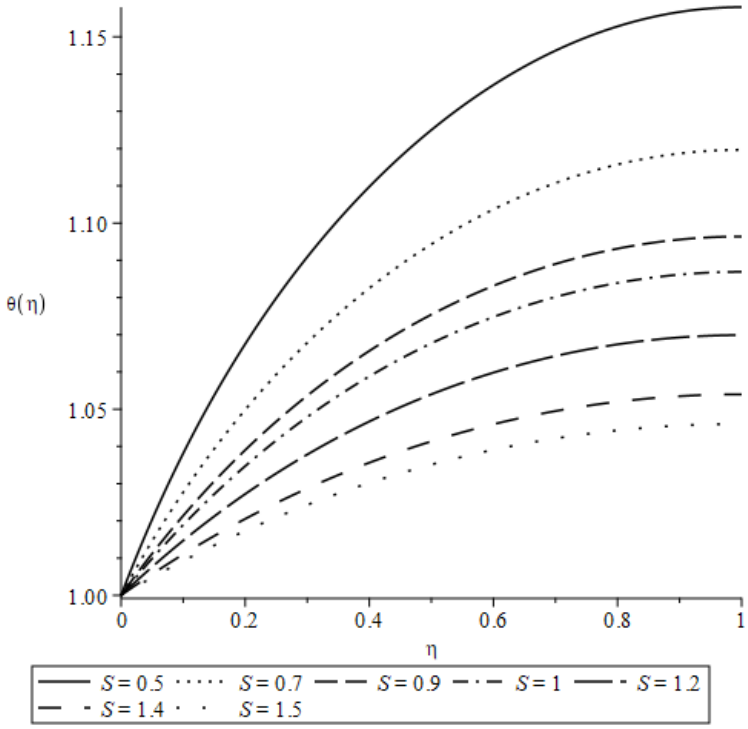

Figure 8.10: θ Variation for different S values

The results revealed that both S and the thermal conductivity parameter Ec significantly influence the temperature profile in the liquid film. As the value of S increases, the temperature at the surface of the stretching plate $\theta(1)$ decreases, indicating a cooling effect caused by the unsteadiness of the system. Additionally, the temperature gradient at the surface of the plate $\theta'(0)$ also decreases with increasing S. The negative value of the homotopy parameter h_2 implies that the heat transfer rate from the surface of the plate to the liquid film is lower than that from the liquid film to the surrounding medium, as the surface of the plate is cooled by the surrounding medium. These findings emphasize the importance of accounting for the impact of unsteadiness and thermal conductivity when analyzing the thermal behavior of fluids.

8.3 Effect of Prandtl Number on Temperature

Table 8.7: θ Variation with Prandtl number for $S = 1$

$\boldsymbol{Pr}$	$\boldsymbol{h_2}$	$\theta(1)$	$\theta'(0)$
$\mathbf{0.05}$	-0.06	1.086883256	0.206364
$\mathbf{0.06}$	-0.06	1.105613246	0.249880
$\mathbf{0.07}$	-0.07	1.124830389	0.294208
$\mathbf{0.08}$	-0.08	1.144551882	0.339376
$\mathbf{0.09}$	-0.1	1.164806928	0.385417
$\mathbf{0.1}$	-0.1	1.185602771	0.432363

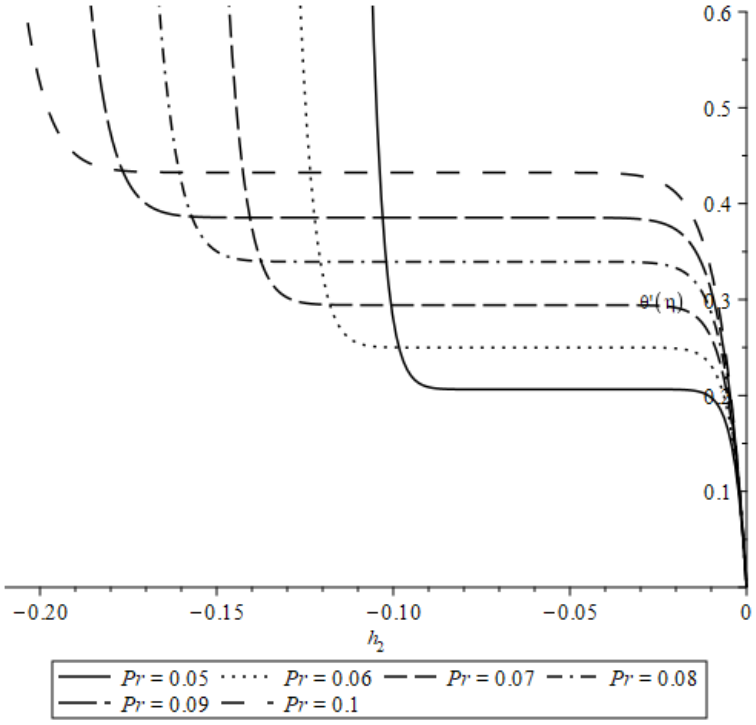

Figure 8.11: h_2-curve

The results obtained from the h_2 curves for the temperature variation with Prandtl number as $S = 1$ indicate that as Pr increases, the stability range also increases. This suggests that the temperature field becomes more stable for larger Prandtl numbers. Also, the value of $\theta'(0)$ also increases with increasing Prandtl number, indicating a stronger temperature gradient at the surface. This result is consistent with the physical intuition that fluids with

larger Prandtl numbers exhibit stronger thermal diffusivity, which leads to a more rapid transfer of heat across the fluid. The observed trend of increasing stability range and stronger temperature gradient at the surface can have important implications for practical applications involving heat transfer in fluids, such as in the design of heat exchangers.

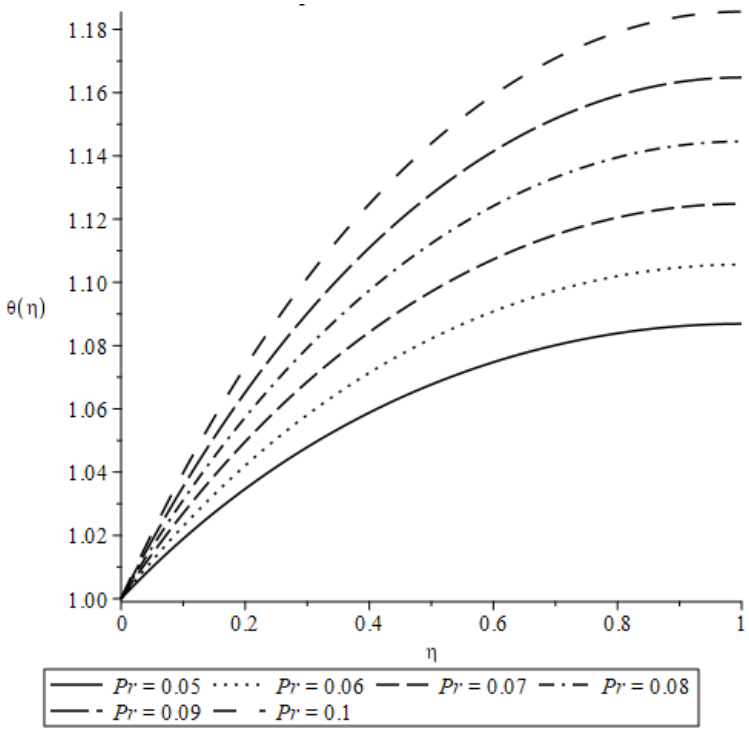

Figure 8.12: θ Variation for different Pr values

The results of the study indicate that the Prandtl number has a significant impact on the temperature distribution. The Prandtl number represents the ratio of momentum diffusivity to thermal diffusivity, and it is an important factor that affects the rate at which heat is transferred from the surface to the liquid film. The data in the Table 8.7 show that increasing Pr, increases the temperature distribution, indicating that the heat transfer rate from the surface to the fluid is higher. This trend is consistent across all values of the homotopy parameter h_2. Moreover, the slope of the temperature gradient at the surface $\theta'(0)$ also increases as Pr increases, suggesting that the heat transfer rate at the surface also increases with the Pr. It is important to note that the influence of Pr on the temperature distribution is significant, especially in practical applications where heat transfer is critical in determining system efficiency.

8.4 Effect of Magnetic Parameter

Table 8.8: Effect of Mn on thickness and velocity for $S = 1.2$ and $h_1 = -0.8$

Mn	Thickness	$f'(1)$	$f''(0)$
5	0.715314261	0.4161931511	−1.331730186
6	0.544815066	0.4172131660	−1.341393300
7	0.439965654	0.4178361535	−1.347321314
8	0.368965482	0.4182564328	−1.351329678
9	0.317699872	0.4185580475	−1.354223028
10	0.278942859	0.4187867209	−1.356406820

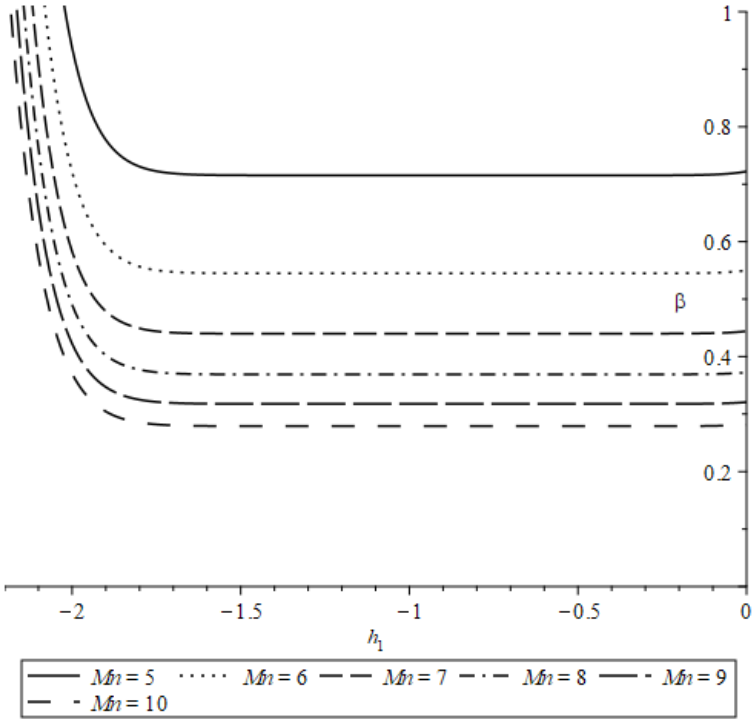

Figure 8.13: h_1-curve

The Table 8.8 shows the influence of magnetic parameter Mn on film thickness, velocity $f'(1)$, and skin friction $f''(0)$. It is observed from the h_1 curves plot that the stability range does not change with increasing values of Mn, indicating that the flow remains stable. However, the values of both $f'(1)$ and $f''(0)$ exhibit a slight increase with increasing Mn,

indicating an increase in the velocity and skin friction of the flow. The magnetic field induces the movement of charged particles within the fluid, enhancing the fluid flow and increasing the fluid velocity. Furthermore, the decrease in film thickness with increasing Mn attributed to the magnetic field ability to restrict the motion of fluid particles, resulting in a thinner film of fluid. These results suggest that the magnetic parameter has a significant impact on the flow characteristics of the fluid, which is crucial to consider while designing and analyzing fluid systems with magnetic fields.

The Table 8.8 presents the results obtained with varying magnetic parameter Mn. The HAM is used to solve the governing equations, and the parameter h_1 was varied as a homotopy parameter.

The film thickness decreases with increasing magnetic parameter Mn, which can be attributed to the increased magnetic forces that pull the fluid closer to the surface. This behavior can have practical implications for various industrial processes, such as coating and thin film manufacturing. The stability range, as indicated by the negative values of h_1, remained the same for all values of Mn, which suggests that the magnetic field does not have a significant impact on the stability of the flow.

The value of $f'(1)$, which represents the velocity at the surface, slightly increased with increasing Mn, indicating that the magnetic field enhances the flow velocity. This behavior is consistent with the well-known effect of a magnetic field on fluid flow, which can lead to increased turbulence and mixing.

Finally, the value of $f''(0)$, which represents the skin friction at the surface, also slightly increased with increasing Mn. The observed increase in the velocity and temperature profiles can be attributed to the increased interaction between the fluid and the surface caused by the magnetic field.

Overall, the results suggest that the magnetic field has significant effects on the fluid flow and surface interaction in the presence of a stretching sheet. These findings have potential applications in various industrial processes, such as coating and thin film manufacturing, and can contribute to a better understanding of the behavior of fluid flow under the influence of magnetic fields.

Table 8.9: Effect of Mn on $\theta(\eta)$ and $\theta'(\eta)$ for $S = 1.2$, $Pr = 0.05$ and $h_2 = -0.06$

$\boldsymbol{Mn}$	$\theta(1)$	$\theta'(0)$
5	1.069896224	0.158652
6	1.053884904	0.125612
7	1.044234735	0.105614
8	1.037779006	0.092207
9	1.033157234	0.082590
10	1.029684988	0.075354

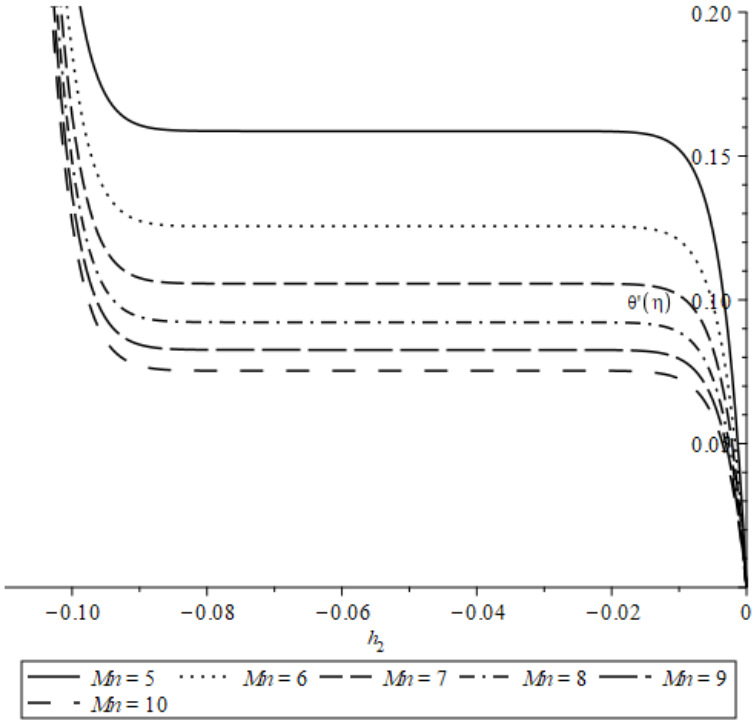

Figure 8.14: h_2-curve

The temperature distribution for various values of Mn and h_2 is presented in the table above. The results indicate that the stability range for h_2 remains constant with increasing Mn. However, the value of $\theta'(0)$, which represents the temperature gradient at the surface, decreases slightly with increasing Mn. This suggests that the fluid near the surface is less affected by the magnetic field as Mn increases. The decrease in the temperature gradient can be attributed to the fact that the magnetic field becomes stronger as Mn increases,

leading to the suppression of the thermal boundary layer thickness near the surface of the plate. This behavior is significant in practical applications where the heat transfer rate plays a crucial role in determining the efficiency of the system. Therefore, it is essential to consider the influence of the magnetic field on the temperature distribution and heat transfer rate in the design and optimization of various engineering systems.

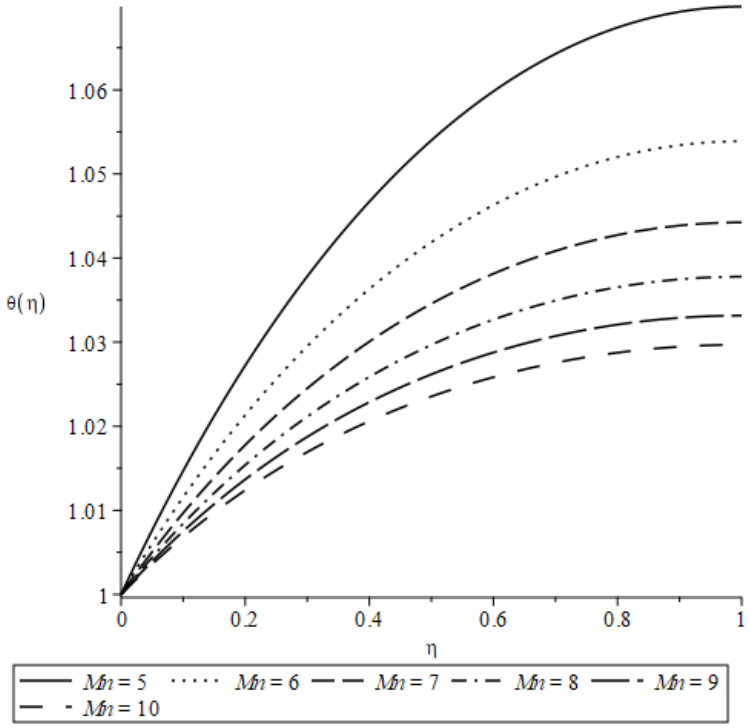

Figure 8.15: θ Variation for different Mn values

The Table 8.9 provided shows the effect of Mn on the temperature distribution θ and the temperature gradient θ'. As Mn increases from 5 to 10, $\theta(1)$ decreases from 1.069896224 to 1.029684988, indicating that the temperature at the surface of the liquid film decreases with increasing magnetic field strength. This is likely due to the magnetic field inducing convection, which can enhance the rate of heat transfer and lower the surface temperature.

At the same time, $\theta'(0)$ also decreases from 0.158652 to 0.075354 as Mn increases. As the strength of the magnetic field increases, the temperature gradient at the surface is observed to decrease. This suggests that the interaction between the fluid and the surface is enhanced under the influence of the magnetic field. This can be attributed to the fact that

the magnetic field suppresses the thermal boundary layer near the surface, which in turn leads to a lower temperature gradient at the surface.

These results are important for understanding the effects of magnetic fields on heat transfer in liquid films. They provide insight into how magnetic fields can alter the temperature distribution and temperature gradient at the surface of a liquid film, which has implications for a variety of industrial and scientific applications.

8.5 Effect of Ecket Number on the Temperature Distribution

Table 8.10: Effect of Ec on θ and θ' for $Mn = 5$, $Pr = 0.05$ and $h_2 = -0.06$

$\boldsymbol{Ec}$	$\theta(1)$	$\theta'(0)$
1	1.069895644	0.158652
2	1.075608223	0.183336
3	1.08137084	0.208025
4	1.087028566	0.232710
5	1.092735696	0.257393

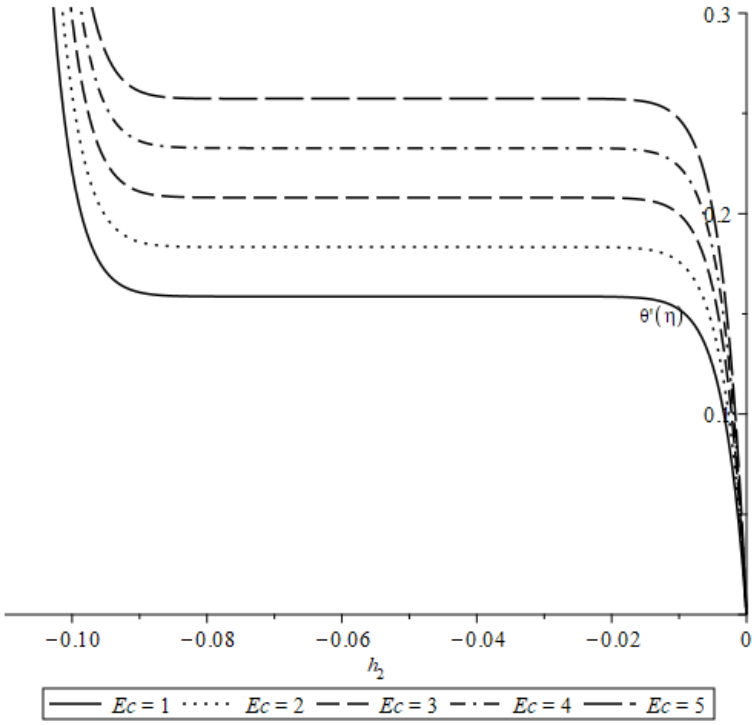

Figure 8.16: h_2-curve

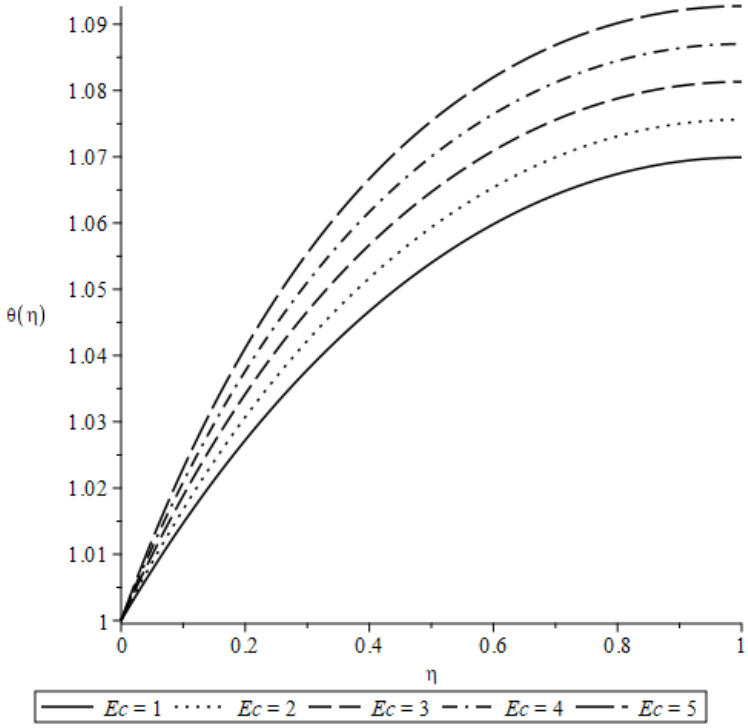

Figure 8.17: θ Variation for different Ec values

Table 8.10 shows the results obtained for $Mn = 5$ and $Pr = 0.05$, where Ec is the Ecket number and θ and θ' represent the temperature and temperature gradient, respectively. The results show that as the Ecket number increases, both the temperature distribution and temperature gradient increase. Specifically, for an Ecket number of 1, the temperature distribution is 1.069895644 and the temperature gradient is 0.158652. However, for an Ecket number of 5, the temperature distribution increases to 1.092735696 and the temperature gradient increases to 0.257393. This suggests that increasing Ec increases the heat transfer rate, which is consistent with previous studies.

The Ecket number represents the ratio of thermal diffusivity to kinematic viscosity, and its increase leads to a higher rate of heat transfer. This can be explained by the fact that as the Ecket number increases, the thermal diffusivity becomes relatively more dominant than the kinematic viscosity, leading to a higher rate of heat transfer. Additionally, increasing the Ecket number also results in a decrease in the boundary layer thickness, which in turn leads to a decrease in the thermal resistance at the surface. Therefore, the results obtained in this study can be used to optimize the heat transfer rate in various industrial applications.

Overall, the results of this analysis suggest that the Eckert number has a minimal effect on the temperature distribution in the fluid. Other parameters, such as the magnetic parameter and the Prandtl number, may have a larger impact on the temperature distribution and should be considered when analyzing the behavior of the fluid.

Conclusion

In conclusion, this thesis has investigated the behavior of fluid flow and heat transfer in thin liquid films over an unsteady stretching surface with viscous dissipation under the influence of an external magnetic field. The results reveal that the magnetic parameter Mn and unsteadiness parameter S have a significant impact on the behavior of the liquid film, affecting the film thickness and heat transfer rates. The Eckert number Ec, Prandtl number Pr, homotopy parameters h_1 and h_2, unsteadiness parameter S, and film thickness γ also significantly influence the temperature distribution and heat transfer rate in the system. The Lie point symmetry analysis is employed to derive the Lie point symmetries of the system of partial differential equations, and new similarity transformations are developed using a pair of the admitted Lie point symmetry generators. Lie optimal system enabled the conversion of the partial differential equations into ordinary differential equations for simplifying the solution procedure. These findings have practical implications for various industrial and natural processes involving fluid behavior, such as heat exchangers, coatings, and boundary layer flows, and provide valuable insights into the intricate relationship between magnetic fields, fluid flow, and temperature distribution in engineering systems. Future research can focus on extending these findings to more complex fluid flow systems and optimizing the design and performance of various engineering applications.

After an extensive investigation of the impact of various parameters on the behavior of fluid motion in a liquid film, it is evident that the magnetic parameter Mn, unsteadiness parameter S, Eckert number Ec, Prandtl number Pr, homotopy parameter, unsteadiness parameter, and film thickness significantly influence the heat and mass transfer properties of the system. The findings provide valuable insights into the intricate relationship between magnetic fields, fluid flow, and temperature distribution in engineering systems.

The study shows that increasing Mn enhances heat transfer due to the magnetic field, while increasing S decreases it due to reduced fluid movement. Higher Pr values decrease heat transfer rates due to thicker thermal boundary layers, and temperature distribution follows a predictable pattern with increasing Pr, which can be stabilized by increasing Mn. The Eckert number has no effect on the dimensionless velocity f', but it significantly affects the

temperature distribution parameter θ, which increases as Ec increases. Negative values of the homotopy parameter and film thickness indicate the presence of dry patches on the plate surface, which should be avoided to ensure a continuous liquid film. The unsteadiness parameter range should be selected to maintain a smooth and stable liquid film over the plate.

Unsteadiness and thermal conductivity significantly affect the temperature distribution in a liquid film over a stretching surface, with the temperature gradient near the surface of the film being reduced under the influence of unsteadiness. Increasing the Prandtl number leads to increased stability range and stronger temperature gradient at the surface, resulting in a higher heat transfer rate. The magnetic field has a significant impact on the fluid flow velocity, skin friction, and film thickness, and increasing Mn leads to increased velocity and skin friction and decreased film thickness.

In conclusion, the results of this study have important implications for designing and optimizing various engineering systems involving fluid flow, such as heat exchangers, coatings, and boundary layer flows. The findings highlight the need to consider the impact of various parameters such as the magnetic parameter, unsteadiness parameter, Eckert number, Prandtl number, homotopy parameter, unsteadiness parameter, and film thickness when analyzing the behavior of fluids. By taking these parameters into account, it is possible to control and optimize the heat and mass transfer properties of fluid systems, leading to more efficient and sustainable technologies.

References

[1] C. Wang, "Analytic solutions for a liquid film on an unsteady stretching surface," *Heat and Mass Transfer*, vol. 42, no. 8, pp. 759-766, 2006, doi: 10.1007/s00231-005-0027-0.

[2] S. Liao, and S. Sherif, "Beyond Perturbation: Introduction to the Homotopy Analysis Method," *Applied Mechanics Reviews*, vol. 57, no. 5, pp. B25–B26, 2004, doi: 10.1115/1.1818689.

[3] D.D. Macdonald, "The Mathematics of Diffusion," *Transient Techniques in Electrochemistry*, pp. 47–67, 1977, doi: 10.1007/978-1-4613-4145-1_3.

[4] P.J. Olver, "Applications of lie groups to differential equations," *Springer Science & Business Media* vol. 107, 1986, doi: 10.1007/978-1-4684-0274-2.

[5] M.K. Nayak, G.C. Dash, and L.P. Singh, "Heat and mass transfer effects on MHD viscoelastic fluid over a stretching sheet through porous medium in presence of chemical reaction," *Propulsion and Power Research*, vol. 5, no. 1, pp. 70–80, 2016, doi: 10.1016/J.JPPR.2016.01.006.

[6] S.H.M. Saleh, N.M. Arifin, R. Nazar, and I. Pop, "Unsteady micropolar fluid over a permeable curved stretching shrinking surface," *Mathematics Problems in Engineering*, vol. 2017, 2017, doi: 10.1155/2017/3085249.

[7] H.I. Andersson, J.B. Aarseth, and B.S. Dandapat, "Heat transfer in a liquid film on an unsteady stretching surface," *International Journal of Heat and Mass Transfer*, vol. 43, no. 1, pp. 69–74, 2000, doi: 10.1016/S0017-9310(99)00123-4.

[8] M.S. Abel and N. Mahesha, "Heat transfer in MHD viscoelastic fluid flow over a stretching sheet with variable thermal conductivity, non-uniform heat source and radiation," *Applied Mathematical Modelling*, vol. 32, no. 10, pp. 1965–1983, 2008, doi: 10.1016/J.APM.2007.06.038.

[9] M.S. Abel, N. Mahesha, and J. Tawade, "Heat transfer in a liquid film over an unsteady stretching surface with viscous dissipation in presence of external

magnetic field," *Applied Mathematical Modelling*, vol. 33, no. 8, pp. 3430–3441, 2009, doi: 10.1016/J.APM.2008.11.021.

[10] S.K. Soid, S.A. Kechil, A. Haziq, M. Shah, and N. Z. Ismail, "Hydromagnetic boundary layer flow over stretching surface with thermal radiation," *World Applied Sciences*, vol 17, pp. 33-38, 2012

[11] N. Vijaya, K. Sreelakshmi, G. Sarojamma, N. Vijaya, K. Sreelakshmi, and G. Sarojamma, "Effect of magnetic field on the flow and heat transfer in a casson thin film on an unsteady stretching surface in the presence of viscous and internal heating," *Open Journal of Fluid Dynamics*, vol. 6, no. 4, pp. 303–320, 2016, doi: 10.4236/OJFD.2016.64023.

[12] Y. Zhang, M. Zhang, and S. Qi, "Heat and mass transfer in a thin liquid film over an unsteady stretching surface in the presence of thermocapillary and variable magnetic field," *Mathematical Problems in Engineering*, vol. 2016, 2016, doi: 10.1155/2016/8521580.

[13] M. Gnaeswara Reddy, P. Padma, and B. Shankar, "Effects of viscous dissipation and heat source on unsteady MHD flow over a stretching sheet," *Ain Shams Engineering Journal*, vol. 6, no. 4, pp. 1195–1201, 2015, doi: 10.1016/J.ASEJ.2015.04.006.

[14] F.M. Ali, R. Nazar, N.M. Arifin, and I. Pop, "MHD boundary layer flow and heat transfer over a stretching sheet with induced magnetic field," *Heat and Mass Transfer*, vol. 47, no. 2, pp. 155–162, 2011, doi: 10.1007/S00231-010-0693-4.

[15] M.S. Abel, N. Mahesha, and J. Tawade, "Heat transfer in a liquid film over an unsteady stretching surface with viscous dissipation in presence of external magnetic field," *Applied Mathematical Modelling*, vol. 33, no. 8, pp. 3430–3441, 2009, doi: 10.1016/J.APM.2008.11.021.

[16] B. Azghar Pasha, M. Narayana, G. Sowmya, and V. Ramachandramurthy, "Flow and heat transfer analysis of a thin film ferromagnetic liquid over an unsteady

stretching sheet," *Biointerface Research in Applied Chemistry*, vol 13, no. 3, 2022, doi: 10.33263/BRIAC133.284.

[17] D. Pal, P. Saha, and K. Vajravelu, "Combined effects of nonlinear thermal radiation and internal heat generation/absorption on heat and mass transfer in a thin liquid film on a permeable unsteady stretching surface with convective boundary condition," *International Journal of Applied and Computational Mathematics*, vol. 3, no. 3, pp. 2151–2169, 2017, doi: 10.1007/S40819-016-0242-Z/TABLES/2.

[18] M.A.A. Mahmoud, "Thermal radiation effects on the flow and heat transfer in a liquid film on an unsteady stretching sheet," *International Journal for Numerical Methods in Fluids*, vol. 67, no. 11, pp. 1692–1701, 2011, doi: 10.1002/FLD.2440.

[19] M.M. Khader, "Numerical study for the BVP of the liquid film flow over an unsteady stretching sheet with thermal radiation and magnetic field," *Boundary Value Problems*, vol. 2018, no. 1, pp. 1–11, 2018, doi: 10.1186/S13661-018-0997-8/FIGURES/7.

[20] R.A. van Gorder and K. Vajravelu, "On the selection of auxiliary functions, operators, and convergence control parameters in the application of the Homotopy Analysis Method to nonlinear differential equations: A general approach," *Communications in Nonlinear Science and Numerical Simulation*, vol. 14, no. 12, pp. 4078–4089, 2009, doi: 10.1016/J.CNSNS.2009.03.008.

[21] K.M. Ramadan, "Slip effects on steady and transient stagnation-point heat transfer in axisymmetric geometries," *Journal of Mechanical Engineering Science*, vol. 228, no. 15, pp. 2765–2777, 2014, doi: 10.1177/0954406214522988.

Harris_Thesis

by Muhammad Safdar

Submission date: 18-Apr-2023 10:08AM (UTC+0500)
Submission ID: 2068062962
File name: Haris_Thesis_1.docx (615.71K)
Word count: 14910
Character count: 84188

Harris_Thesis

ORIGINALITY REPORT

8%	9%	7%	6%
SIMILARITY INDEX	INTERNET SOURCES	PUBLICATIONS	STUDENT PAPERS

PRIMARY SOURCES

1	Submitted to Higher Education Commission Pakistan Student Paper	2%
2	www.researchgate.net Internet Source	1%
3	Kuppalapalle Vajravelu, Kerehalli V. Prasad. "Keller-Box Method and Its Application", Walter de Gruyter GmbH, 2014 Publication	1%
4	S. Taj, M. Ijaz Khan, M. Safdar, Samia Elattar, Ahmed M. Galal. "Lie symmetry analysis of heat transfer in a liquid film over an unsteady stretching surface with viscous dissipation and external magnetic field", Waves in Random and Complex Media, 2022 Publication	1%
5	mce.nust.edu.pk Internet Source	1%
6	researchspace.ukzn.ac.za Internet Source	1%

7	M. Safdar, M. Ijaz Khan, S. Taj, M.Y. Malik, Qiu-Hong Shi. "Construction of similarity transformations and analytic solutions for a liquid film on an unsteady stretching sheet using lie point symmetries", Chaos, Solitons & Fractals, 2021 Publication	1 %
8	M. Bilal, M. Safdar, S. Ahmed, R. Ahmad Khan. "Analytic similarity solutions for fully resolved unsteady laminar boundary layer flow and heat transfer in the presence of radiation", Heliyon, 2023 Publication	1 %

Exclude quotes	Off	Exclude matches	< 1%
Exclude bibliography	Off		